SOILS AND FOUNDATIONS Vol. 43, No. 2, 33-54, April 2003
Japanese Geotechnical Society

# IMPROVING THE DYNAMIC PERFORMANCE OF PRELOADED AND PRESTRESSED MECHANICALLY REINFORCED BACKFILL BY USING A RATCHET CONNECTION

MASAHIRO SHINODA[i], TARO UCHIDA[ii] and FUMIO TATSUOKA[iii]

## ABSTRACT

A series of laboratory model shaking table tests were performed to evaluate improvement of the dynamic performance of mechanically reinforced soil structures that are vertically preloaded and prestressed by using a ratchet connection for the tie rods. The preloading and prestressing (PLPS) procedure was originally developed to substantially decrease the residual settlement at the top of backfill subjected to long-term live load such as traffic load. It is shown that the maintenance of high prestress in the backfill is also essential to substantially reduce the shear and bending deformation as well as vertical compression of reinforced backfill subjected to dynamic load. For relatively slender reinforced backfill structures, the maintenance of high prestress is particularly important to restrain the occurrence of large bending deformation of backfill. For these purposes, it is proposed that the top end of the tie rods be fixed to the crest of the structure by using a ratchet connection, which allows free compression of backfill at nearly constant prestress while mechanically not allowing any expansion of backfill. It is suggested that, to avoid a resonant or near-resonant state during seismic loading, the initial value of the natural frequency $f_n$ of a given structure be designed to be sufficiently higher than the anticipated predominant frequency $f_p$ of given seismic load, while the $f_n$ value during dynamic loading is maintained at a higher valve than the $f_p$ value by using a ratchet connection.

**Key words:** earthquake resistance, model test, preloading, prestressing, ratchet connection, reinforced soil, shaking table test (IGC: E8/E12/K14)

## INTRODUCTION

When a mechanically reinforced backfill structure, such as a geosynthetic-reinforced soil retaining wall (GRS RW), is subjected to seismic load, the active zone in the backfill, located adjacent to the wall face, displaces outwards more than the more stable zone located in the back of the potential failure zone. For this reason, horizontally placed tensile reinforcement layers extending from the active zone into the stable zone can contribute to the seismic stability of mechanically reinforced backfill structures. It is also very effective to use a full-height rigid facing or a segmental block facing, and to connect the reinforcement layers to the back of the facing to increase the seismic stability of reinforced soil RWs. Both techniques have been validated by high seismic performance of a number of reinforced soil RWs of this type during recent severe earthquakes, including the 1995 Hyogoken-Nambu Earthquake (Tatsuoka et al., 1996, 1997b, c) and the 1995 Northridge Earthquake (e.g. White and Holtz, 1997). Results from a set of laboratory model shaking table tests support the above (e.g., Murata et al., 1994; Koseki et al., 1997; Bathurst and Alfaro, 1998; Tatsuoka et al., 1998).

However, despite this, it has been noted that simple shear deformation with essentially zero horizontal normal strain, which is another fundamental mode of global deformation of reinforced backfill subjected to high seismic load, should be minimised to achieve a high seismic stability of the structure. Horizontally placed tensile reinforcement layers cannot efficiently restrain this mode of deformation even if the stiffness of reinforcement is very high. One of the most efficient ways to avoid this mode of deformation is to increase the shear stiffness of backfill by vertical prestressing (Tatsuoka et al., 1998).

In the meantime, a preloading and prestressing (PLPS) construction procedure has been proposed to substantially reduce the transient and residual vertical compression of mechanically reinforced backfill structures subjected to long-term live load such as traffic load (Fig. 1; Tatsuoka et al., 1997a, b). In the PLPS procedure, a relatively high vertical preload is applied to reinforced backfill by using a set of tie rods (usually four), which is then partially unloaded to make the deformation of backfill essentially elastic against external vertical loading at the crest of the structure. A very high preload could be applied as the backfill is reinforced. The bottom end of the tie rods are fixed to a RC reaction block constructed im-

[i] Research Engineer, Integrated Geotechnology Institute Limited, formerly Graduate Student, University of Tokyo.
[ii] Research Assistant, University of Tokyo.
[iii] Professor, ditto.
Manuscript was received for review on October 22, 2001.
Written discussions on this paper should be submitted before November 1, 2003 to the Japanese Geotechnical Society, Sugayama Bldg. 4F, Kanda Awaji-cho 2-23, Chiyoda-ku, Tokyo 101-0063, Japan. Upon request the closing date may be extended one month.

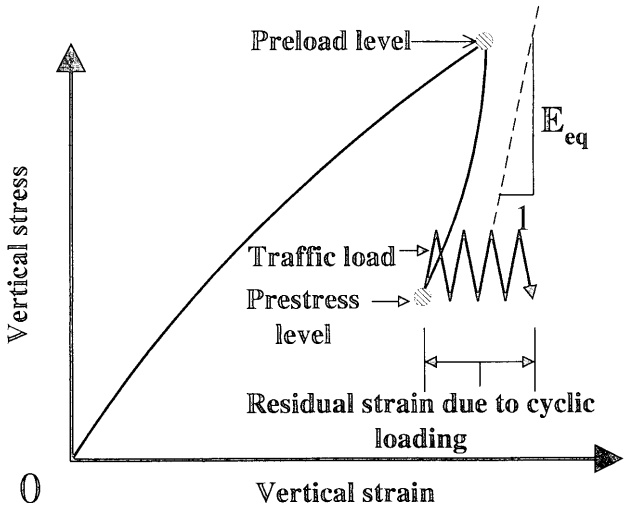


**Fig. 1. Schematic diagram showing the behaviour of backfill during preloading, unloading and cyclic loading at prestressed state**

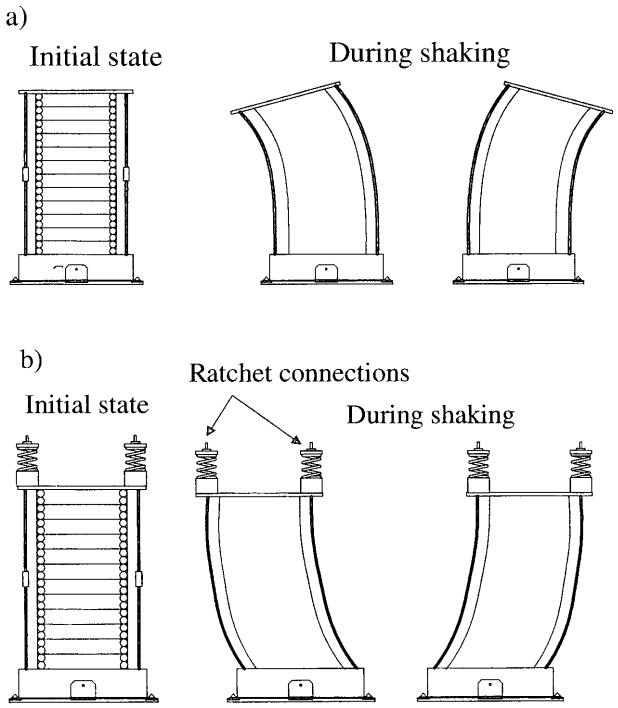


**Fig. 2. Typical deformation of PLPS reinforced soil structure: a) bending deformation after prestress has decreased to a very low level, and b) restraining of bending deformation by using ratchet connections**

mediately below the bottom of the backfill or anchored in the subsoil below the backfill, while the top ends are fixed to a RC reaction block on the crest of the backfill, which may also be used as a foundation for a bridge girder. After this stage, the prestress remaining in the backfill is in equilibrium with the tie rod tension. It was found that relaxation of the tie rod tension could be made very small by a relevant preloading procedure (Shinoda et al., 2001a; Uchimura et al., 1998, 2001, 2002; Tatsuoka et al., 2000, 2001a, b, c). The behaviour of a proto-type preloaded and prestressed backfill bridge pier (Uchimura et al., 1996, 1998, 2001) and results from comprehensive model loading tests (Shinoda et al., 1999, 2001a) have shown that the transient and residual compression of backfill subjected to vertical cyclic loading can be made very small when the initial prestress level is about half of the preload level, while the difference between the preload level and the initial prestress level is sufficiently larger than the applied external vertical load, say by a factor of two or more. It has also been found that to ensure a high performance of PLPS backfill while the structure is in service, prestress in the backfill should be maintained to a sufficiently high level.

Shinoda et al. (2000a, b) showed that sufficiently high prestress is also essential to keep the shear deformation of backfill very small when subjected to seismic load. When such a PLPS reinforced soil structure as above is slender and the initial prestress is too low, the structure may exhibit large bending deformation when subjected to a high-level seismic load (Fig. 2(a)). In that case, the height at both sides of PLPS reinforced soil structure may largely increase and decrease cyclically. When the height of backfill increases largely, the vertical stresses in that backfill may become temporarily very low or even nearly zero. Then, the shear strength and stiffness in the backfill may become very low, resulting in excessive shear deformation of backfill. For this reason, it is necessary to keep sufficiently small the bending deformation of PLPS reinforced backfill structure during seismic loading by some measures.

In view of the above, a series of static cyclic lateral loading tests (Kikuchi et al., 1999; Uchimura et al., 2002) and shaking table tests were performed on scaled models in the authors' laboratory to evaluate the seismic stability of relatively slender PLPS geosynthetic-reinforced soil (GRS) structures and to find an effective method to substantially improve the dynamic performance of such structures. These static and dynamic loading tests were performed on the same types of models as those used in another series of model tests performed to evaluate the effects of the PLPS procedure on the transient and residual vertical compression of backfill subjected to vertical cyclic loading with a large number of cycles, such as traffic load (Shinoda et al., 1999, 2001a). Reported herein are results from a series of shaking table model tests performed using a well-graded gravel as the backfill. Results from these model tests showed that to maintain as high as possible prestress during dynamic loading and to prevent the increase in the height of backfill, it is effective to use a new device, called the ratchet connection, to fix the top end of tie rods to the crest of the structure. Results from similar tests performed using Toyoura sand have been reported by Shinoda et al. (2000a, b).

## TEST METHOD

*Models and Measuring System*

Models were 55 cm-high and 35 cm by 35 cm in cross-section (Figs. 3(a), (b), (c)). Such relatively slender

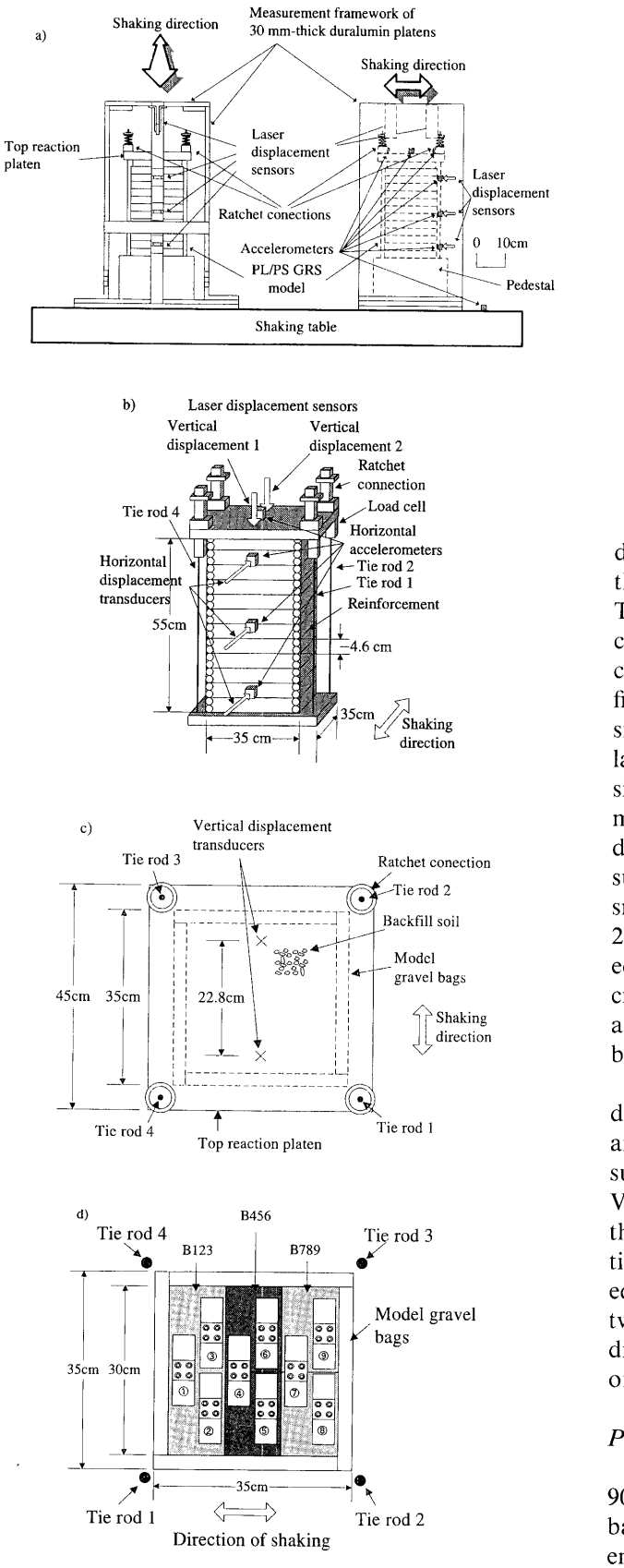


**Fig. 3. Grain size distribution curve of the gravel for the backfill**
**a) General view of a PLPS GRS structure model on a shaking table**
**b) PLPS GRS model with measurement systems**
**c) Top view of model**
**d) Arrangement of local two-component load cells at the bottom of backfill**

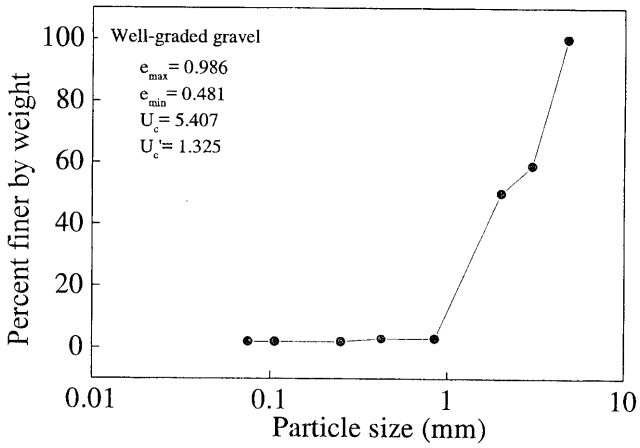


**Fig. 4. Grain size distribution curve of the gravel for the backfill**

dimensions as above were selected to critically investigate the seismic stability of PLPS reinforced soil structures. The backfill of the models was a well-graded gravel of crushed sandstone ($D_{50}=2.52$ mm; $U_c=5.41$; zero fines content; $e_{max}=0.986$; and $e_{min}=0.481$; Fig. 4). The backfill was compacted by manual tamping to a relative density of 90% in 12 sub-layers and reinforced with 12 grid layers at a vertical spacing of 4.6 cm. Each grid layer consisted of 34 phosphor bronze strips (3.5 mm-wide, 0.2 mm-thick and 350 mm-long), 17 in each perpendicular direction, with an aperture of 8 mm. The edge of each sub-layer of backfill was protected with two layers of small gravel-filled fabric bags having a diameter of about 2.3 cm. The end of each reinforcement layer was connected to the respective gravel bags. A square steel plate of 5 cm in thickness and 45 cm by 45 cm in cross-section with a weight of 282 N was placed on the top of the reinforced backfill.

Horizontal accelerometers and displacement transducers were set with targets being located on the top plate and the mid-heights of the second, sixth and eleventh sub-layers from the bottom of the backfill (Fig. 3(b)). Vertical displacements were measured at two places on the top plate to obtain average height changes and rotations at the crest of the model (Fig. 3(c)). Each tie rod was equipped with a load cell to measure tension, while nine two-component load cells were arranged to measure the distributions of shear and normal stresses at the bottom of the backfill (not including the gravel bags) (Fig. 3(d)).

*Preloading and Prestressing of the Backfill*

An average vertical stress of either 30 kPa or 60 kPa or 90 kPa as preload (PL) was first applied to the top of the backfill by using four steel tie rods. The top and bottom ends of the tie rods were fixed to the top reaction steel plate and to the pedestal of the model. The average vertical stress applied by using four tie rods was then decreased to the prescribed initial prestress (PS), which was either 15 kPa or 30 kPa or 45 kPa. The ratio of PL to PS was equal to 2.0, which was found to be effective in minimizing the residual vertical compression of backfill

subjected to long-term vertical cyclic loading simulating traffic load (Shinoda et al., 1999, 2001a). These PL and PS levels were determined as follows:

1) It was assumed that the scale of model be smaller by one sixth of magnitude than that of prototype PLPS GRS structures.
2) To make the dynamic behaviour of the model representative of that of the prototype structures, the ratio of "the vertical stresses applied to the model" to "the horizontal dynamic force acting on the model responding to the input horizontal motion" was set similar to the corresponding ratio with the prototype structures.
3) A horizontal acceleration level of a similar order of magnitude as the highest peak horizontal ground acceleration (PGA) recorded during the 1995 Hyogoken-Nambu Earthquake (i.e., of the order of 700 gals) was applied to the model.
4) From terms 1) through 3), "the horizontal dynamic force acting on the model" became one six of the value of the prototype structures and, therefore, "the vertical stresses applied to the model" should be smaller by a factor of six than the values for the prototype structures.
5) A prototype preloaded and prestressed bridge pier was constructed in 1996 (Uchimura et al., 1996, 1998, 2001; Shinoda et al., 2001a). The dimensions were 2.7 m high, 4.4 m by 6.4 m in cross-section at the base and 2.4 m by 5.0 m in cross-section at the crest. The PL value applied to the reinforced backfill was 196 kPa when the applied load was averaged for the cross-sectional area of the reaction block (equal to 12 $m^2$) and 107 kPa when the applied load was averaged for the cross-sectional area of the backfill (equal to 22 $m^2$), while the corresponding initial PS value was 82 kPa and 45 kPa. It is preferred and quite feasible to increase these PL and PS levels by a factor of two to support heavier dead and live load; i.e., PL = 200 kPa and initial PS = 100 kPa (averaged for the cross-sectional area of the backfill).
6) Therefore, as PL and initial PS values, the vertical stresses averaged for the cross-sectional area of the backfill, equal to 30 kPa and 15 kPa, correspond to 180 kPa and 90 kPa respectively of the prototype structures. To evaluate the effects of PL and initial PS levels, PL and initial PS values higher than respectively 30 kPa and 15 kPa were also employed.

On the other hand, to evaluate the effects of the PLPS procedure on the transient and residual compression of reinforced backfill by long-term vertical cyclic loading, Shinoda et al. (2001a) performed another series of model tests, in which model dimensions and other configurations were the same as those in the present study. In those tests, an average vertical stress ranging from 100 kPa to 250 kPa, which is higher than those employed in the present study, was applied at the preloading stage. This is because, in those model tests, the ratio of the cyclic vertical stress to the vertical stress at the preloading and prestressing stages which is similar to typical values of prototype structures was employed while using cyclic vertical stresses which are typical of prototype structures.

*Dynamic Loading*

About 100 cycles of sinusoidal waves with a peak horizontal acceleration of 700 gals and a frequency $f_i$ of either 5 Hz or 10 Hz, having an initial stage where the input acceleration level increased linearly up to the stationary value, were applied to the table. This high input motion was chosen to examine whether PLPS GRS structures can survive without exhibiting serious structural damage under such very high seismic load as experienced during the 1995 Hyogoken-Nambu Earthquake. The highest peak ground horizontal acceleration (PGA) recorded during this earthquake was of the order of 700 gals (JGS, 1996), and this order of PGA is specified as the design value in many aseismic design codes for civil engineering structures in Japan.

The natural frequency $f_n$ at very small strains (smaller than 0.001%) in the backfill of the prototype PLPS GRS bridge pier described above was measured by giving lateral impact to the structure (Nakarai et al., 2000). The $f_n$ value was of the order of 7 Hz in the longer direction (perpendicular to the bridge axis) and 9 Hz in the shorter direction (parallel to the bridge axis). The $f_n$ value of such structures decreases with an increase in the height-to-width ratio of the structure. In the present study, prototype PLPS GRS structures that are more slender than this prototype pier, were considered as typical ones. These prototype structures should then have smaller $f_n$ values. According to the theoretical analysis described later in this paper, when the height increases to 3.3 m (with $\lambda = 6$ for the models in the present study), the $f_n$ value should decrease to 4.6–6.2 Hz under otherwise same conditions. These $f_n$ values are much larger than the predominant frequency $f_p$ of the strong horizontal motions recorded at the ground surface during the 1995 Hyogoken-Nambu Earthquake, equal to the order of 1–3 Hz (JGS, 1996). Therefore, it is very likely that these prototype structures would not have exhibited a resonance if they had been subjected to strong horizontal motions during the 1995 Hyogoken-Nambu Earthquake. In view of the above, in the present study, the frequency $f_i$ of the input sinusoidal motion was set to be smaller than measured natural frequencies $f_n$ at small strains of the models, as in the case of the considered prototype structures (i.e., $f_p$ = 1–3 Hz versus $f_n$ = 4.6–6.2 Hz).

The natural frequencies $f_n$ at small strains (of the order of 0.01%) for the first mode of deformation of each model were evaluated by performing sweep tests with an acceleration of 100 gals at a changing rate of frequency equal to 0.5 Hz/sec. The following $f_n$ values were obtained under nearly constant prestress conditions (which were realized by using the ratchet connection explained below):

—$f_n$ = 6.5 Hz when the tie rod tensions were zero (i.e., when PL = PS = 0 kPa) (this model was not subjected to an acceleration level of 700 gals);
—$f_n$ = 10.5 Hz when PL = 30 kPa and PS = 15 kPa;

—$f_n$ = 11.4 Hz when PL = 60 kPa and PS = 30 kPa; and
—$f_n$ = 12.3 Hz when PL = 90 kPa and PS = 45 kPa.
Therefore, a frequency $f_i$ = 5 Hz of the input sinusoidal motion, which was much smaller than "the natural frequencies at small strains of the models" (for PS = 15 − 45 kPa) $f_n \cong$ 10–12 Hz, was chosen so that the model would not resonate to the input motion as long as the prestress did not become very small during dynamic loading. Related considerations based on the similitude rule are given in Appendix A.

On the other hand, when the initial natural frequency $f_n$ of a model is only marginally higher than the $f_i$ value of the input motion, an increase in the input motion level causes the $f_n$ value to decrease and it can approach the $f_i$ value due to effects of the strain-non-linearity on the stiffness of backfill and a large decrease in the prestress during shaking. A frequency $f_i$ = 10 Hz of the input motion, which was only marginally smaller than these natural frequencies $f_n$, was also chosen to evaluate the dynamic behaviour of PLPS GRS structures at the resonant condition (i.e., the worst scenario in terms of dynamic response of structure).

The following remarks are relevant to present dynamic loading tests:

1) With respect to the damage level caused by dynamic loading for civil engineering structures, the input sinusoidal motion with a peak acceleration of 700 gals used in the present study would be much severer than a natural seismic motion with a PGA of 700 gals (e.g., Bathurst and Hatami, 1998; Hatami and Bathurst, 2001).
2) Resonance can also be avoided by making the initial natural frequency $f_n$ of the structure sufficiently lower than the $f_p$ value of random input motion or the $f_i$ value of sinusoidal input motion. However, the efficiency of this method could be reduced by too large cyclic deformation, which may damage the structure seriously.

Two series of dynamic loading tests were performed using input frequencies $f_i$ = 5 Hz and 10 Hz. In each series, the following three types of tie rod connection were used:

1) *Rigid connection:* The tie rods were fixed rigidly to the top reaction plate by using nuts in place of the ratchet connections shown in Fig. 3(a). Due to a relatively high stiffness of the steel tie rods ($K_1$ = about 1,100 N/mm for a single tie rod), the tie rod tension decreased at a very high rate when the backfill exhibited vertical compression. For a model having an initial natural frequency $f_n$ equal to about 10 Hz, when $f_i$ = 5 Hz, a rapid and significant decrease in the $f_n$ value during cyclic loading would result in a transient resonance, which could result in excessive deformation of the model.
2) *Constant stress connection:* The top end of each tie rod was fixed to the top reaction plate by using a metal spring having a relatively low stiffness ($K_2$ = about 5 N/mm for a single spring) to keep the prestress as constant as possible even when the backfill exhibits some compression in the course of shaking. This arrangement allows for an increase in the height of backfill, inducing some bending deformation of backfill. As shown later, due to some viscous resistance against deformation inside the springs, the spring force increased and decreased to some extent in each cycle of shaking according to trends of, respectively, increase or decrease in the backfill height.
3) *Ratchet connection:* The top end of each tie rod was fixed to the top reaction plate by using a ratchet system as shown in Figs. 3(a) and (b), which is explained in detail below.

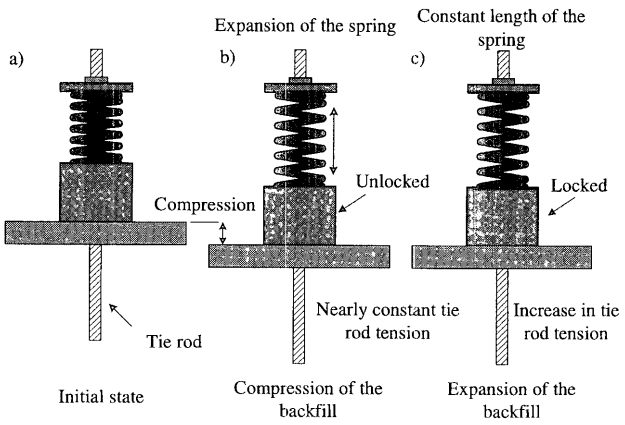


**Fig. 5. Two different functions of the ratchet connection for tie rods**

*Ratchet Connection System (Fig. 5(a))*

Figure 2(b) shows schematically the behaviour of a backfill during dynamic loading when a ratchet connection system is used. When the backfill height tends to decrease due to creep deformation or shaking-induced transient and residual compression or bending deformation of backfill (Fig. 2(a)), the ratchet connection is unlocked while the length of a relatively long and relatively soft spring attached between the top end of each tie rod and the top reaction plate increases (Fig. 5(b)). In this way, the stiffness of each tie rod system becomes very low while keeping the prestress level high, close to the initial value. On the other hand, when the backfill height tends to increase due to dilatancy (i.e., irreversible volume increase by irreversible shear deformation) of backfill during monotonic or cyclic loading or the bending deformation of backfill, the ratchet connection locks (Figs. 2(b) and 5(c)), which makes the stiffness of the tie rod system very high, exerting the original stiffness of the tie rods while largely increasing tie rod tension. By the two functions of the ratchet system described above, the bending deformation of structure can be effectively restrained, as illustrated in Fig. 2(b) (and as shown below). Shinoda et al. (2001b) reported the mechanical details of the ratchet connection.

Figure 6 shows the relationship between the axial force and the axial elongation of a single ratchet connection system (without using a tie rod) used in the present study

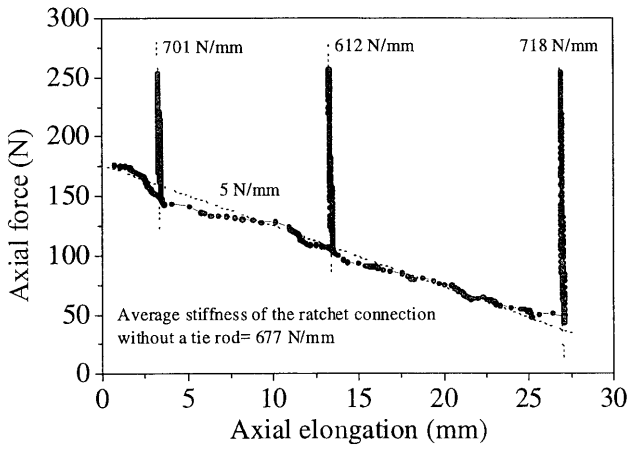


**Fig. 6. Relationships between axial force and axial elongation of the ratchet connection used in the present study**

that was obtained from a stress-controlled calibration test. This is equivalent to the relationship between the tie rod tension and the vertical compression of the model backfill equipped with a ratchet connection. The following trends of behaviour may be seen from Fig. 6:

1) When the ratchet is unlocked (as shown in Fig. 5(b)), the axial force decreases at a very low rate of about 5 N/mm with an increase in axial elongation, which is nearly the same with stiffness $K_2$ (=5 N/mm) of the spring.
2) When the ratchet is locked (as shown in Fig. 5(c)), the axial force increases at a very high rate of 677 N/mm, on average, as the axial length is forced to decrease. When the axial length of the ratchet system is subsequently forced to increase, the tie rod tension decreases at a very high rate in the same way as when the axial length of the ratchet system is forced to decrease until rejoining the primary relationship that is controlled by the stiffness of the spring.

In the model test, the stiffness $K$ of the tie rod system is also controlled by the stiffness of the four tie rods ($K_1$ = about 1,100 N/mm for a single tie rod) and the stiffness of the ratchet system ($K_2$ = about 5 N/mm for a single spring in unlocked condition; $K_3$ = about 677 N/mm for a single ratchet system in locked condition). The theoretical values of the stiffness of the tie rod system when the ratchet system is locked and unlocked are therefore $K = 4/(1/K_1 + 1/K_3) = 1676$ N/mm and $K = 4/(1/K_1 + 1/K_2) = 20$ N/mm.

## TEST RESULTS ($f_i$ = 5 Hz)

*Effect of the Use of Ratchet Connection*

The top three records in Fig. 7(a) are the time histories of horizontal acceleration at the top plate and input motion at the shaking table obtained from three tests with PL = 30 kPa and an initial PS = 15 kPa performed at $f_1$ = 5 Hz. Figures 7(b) through e show the time histories of averaged vertical compressive strain of the backfill, rotation angle of the top plate, average shear strain of the backfill (equal to lateral displacement at the crest of the backfill divided by the backfill height), and average vertical stress acting at the crest of the backfill. Note that the average vertical stress values presented in Fig. 7(e) and in the other similar figures are the values acting at the top of the backfill, which is equal to the sum of the following two components, such as 1)+2) or 1)+3):

1) the average vertical stress applied by using four tie rods, equal to the total tie rod tension divided by the cross-sectional area of backfill, which is denoted as the prestress (PS);
2) the weight of the top reaction plate without a ratchet system divided by the cross-sectional area of backfill, which is equal to 3.5 kPa; or
3) the weight of the top reaction plate with four ratchet systems divided by the cross-sectional area of backfill, which is equal to 4.3 kPa.

For this reason, the initial vertical stress when PS = 15 kPa is equal to 18.5 kPa for a rigid connection and 19.3 kPa for a ratchet connection. The following trends of behaviour may be seen from these figures:

1) The behaviour of the model with a rigid connection changed largely during shaking, as described below, due to a large change in the natural frequency ($f_n$) of the model caused by a large loss of vertical stress and an associated increase in the shear strain in the backfill:
   a) At the initial stage before the elapsed time ($t$) became about 3.5 seconds, the average prestress increased temporarily two times in each cycle of shaking in a similar way to the test with a ratchet connection (Fig. 7(e)). It is likely that this trend of behaviour was due mostly to the bending deformation of backfill and partly to the dilatancy of backfill. This rather stable behaviour was because the tie rods had not largely loosened yet and therefore could effectively restrain the expansion of backfill. The vertical strain of backfill (Fig. 7(b)), the rotation of the top plate (Fig. 7(c)) and the average shear strain of backfill (Fig. 7(d)) were kept relatively small.
   b) The lower bound of the vertical stress started decreasing immediately after the start of shaking. By $t$ = 5 seconds, both peak and lower bounds of the vertical stress had become very small, nearly equal to the value solely induced by the weight of the top reaction plate (Fig. 7(e)). Correspondingly, by $t$ = 5 seconds, the rotation of the top plate had become very large (Fig. 7(c)), indicating that the bending deformation of backfill had become very large. This behaviour was due to (1) the tie rods becoming unable to effectively restrain the expansion of backfill because of full loosening of the tie rods; and (2) the stiffness of backfill becoming very small due to a substantial decrease in the vertical stress in the backfill. The second factor resulted in very large shear strains of the backfill (Fig. 7(d)). The large bending and shear defor-

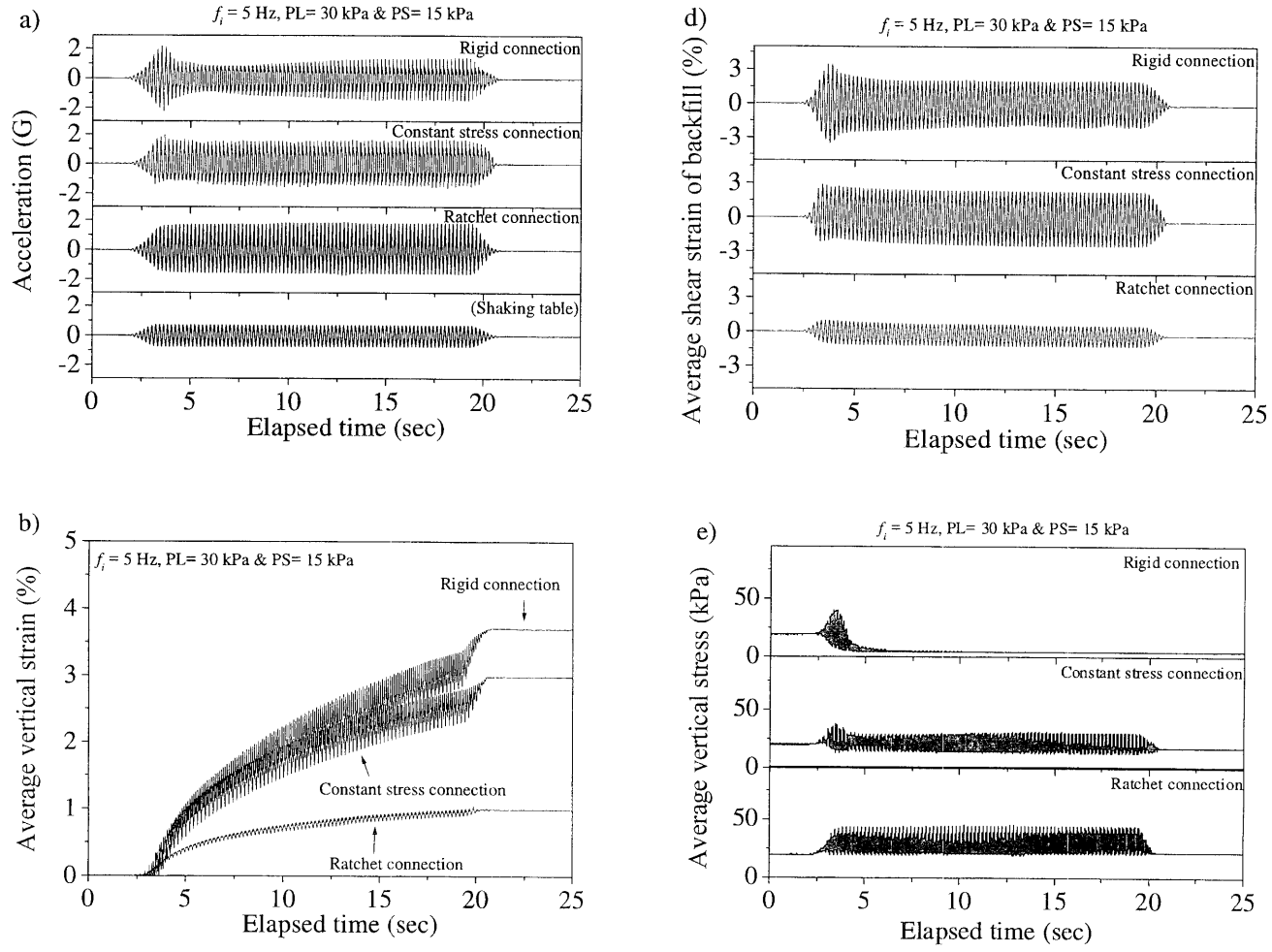


**Fig. 7. Time histories of: a) horizontal acceleration at the top platen (the top three) and the table (the bottom), b) average vertical strain of backfill, c) rotation of the top platen, d) average shear strain of backfill, and e) average prestress, from three tests with rigid, constant stress and ratchet connection (PL = 30 kPa and PS = 15 kPa, $f_i$ = 5 Hz)**

mation of backfill, which continued until the end of the shaking, resulted in large ultimate residual vertical compression of backfill (Fig. 7(b)).

c) At $t$ = 3.6 seconds, the ratio of acceleration between the top and bottom of the model temporarily exhibited a maximum value, showing a transient resonant state. This was caused by a continuous drop of the natural frequency of the model due to a continuous drop in the vertical stress (i.e., a continuous drop in the tie rod tension) and an associated increase in the shear strain in the backfill.

2) At the initial stage of shaking, the model with a constant stress connection exhibited the largest rotation of the top plate among the three models (Fig. 7(c)), because the constant stress connection could not effectively restrain the expansion of backfill. The different trends of behaviour at the initial stage between the models with rigid and constant stress connections indicate that the use of stiff tie rods is effective to restrain the bending deformation of backfill as long as the tie rod tension is kept high enough. The same conclusion was obtained from a series of static cyclic lateral loading tests on the same type of models using Toyoura sand backfill (Kikuchi et al., 1999; Uchimura et al., 2002).

3) With a constant stress connection, the average vertical stress was kept rather constant throughout the shaking (Fig. 7(e)), while the rotation angle of the top reaction plate (Fig. 7(c)) and the shear strain of

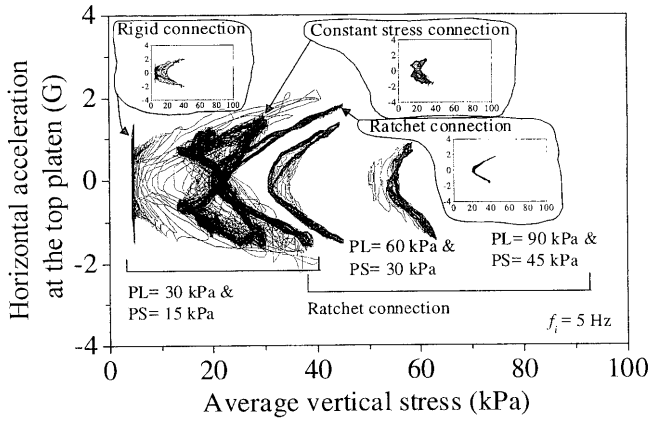


**Fig. 8. Relationships between horizontal acceleration at the top platen and average prestress, from three tests (PL = 30 kPa and PS = 15 kPa; $f_i$ = 5 Hz) and the other two tests with a ratchet connection (PL = 60 kPa and PS = 30 kPa, PL = 90 kPa and PS = 45 kPa; $f_i$ = 5 Hz)**

backfill (Fig. 7(d)) were also rather constant and relatively large. Correspondingly, relatively large bending deformation of backfill associated with this behaviour resulted in relatively large ultimate residual vertical compression of backfill (Fig. 7(b)). The vertical stress decreased and increased in an unsystematic way in each cycle (Fig. 7(e)), which was likely due to a variable resistance of the spring against deformation.

4) The model with a ratchet connection exhibited substantially smaller rotation of the top plate (Fig. 7(c)) and shear deformation of the backfill (Fig. 7(d)) throughout the shaking as compared with the other two models. The ultimate residual compression of backfill was also much smaller (Fig. 7(b)). Importantly, the lower bound of the average vertical stress did not become lower than the initial value throughout the shaking, while the peak prestress became temporarily very large two times in each cycle of shaking when the expansion of backfill was restrained by the tie rods having a high stiffness (Fig. 7(e)).

To confirm the advantages of using a ratchet connection, the behaviour of the three models is compared in more detail below. Figure 8 compares the relationships between the horizontal acceleration at the top plate and the average vertical stress at the top of the backfill, which is indicative of the relationship between the shear and vertical stresses acting inside the backfill (i.e., a sort of stress path). For clarity, the relationship in each case is also indicated in the respective inset small figure. The stress paths from an other two tests using a ratchet connection with PL = 60 and 90 kPa are also presented in this figure, which will be explained later. It may be seen that, in the all the tests, the average vertical stress increased two times as the horizontal acceleration at the backfill increased in the opposite direction in each cycle of shaking. Importantly, the average vertical stress in the model with a ratchet connection did not become smaller than the initial

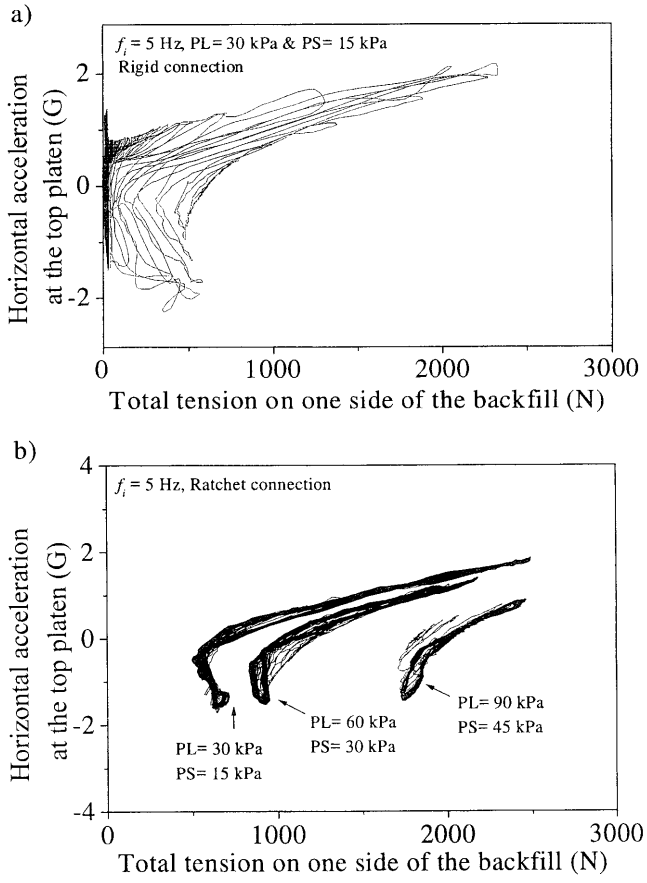


**Fig. 9. Relationships between horizontal acceleration at the top platen and total tension in a pair of tie rods on one side of backfill: a) the model with a rigid connection (PL = 30 kPa and PS = 15 kPa; $f_i$ = 5 Hz), and b) three tests with a ratchet connection (PL = 30 kPa and PS = 15 kPa, PL = 60 kPa and PS = 30 kPa, PL = 90 kPa and PS = 45 kPa; $f_i$ = 5 Hz)**

value at any moment during shaking. The shape of the stress path reflects the dilatancy characteristics of backfill (like the one in undrained simple shear tests on saturated sand).

Figures 9(a) and (b) show the relationships between the horizontal acceleration at the top reaction plate and the total tension in a pair of tie rods located on one side of backfill obtained from four tests on the models with rigid and ratchet connections. It may be seen that the variation of the total tension in a pair of tie rods on each side of backfill was not symmetrical about the axis of horizontal acceleration. The tie rod tension on the backside of the shaking direction increased largely by restraining the increase in the height of backfill on the backside of shaking, which was due mostly to the bending deformation of backfill and partly to the dilatancy of backfill. On the other hand, the increase in the tie rod tension was relatively small on the front side of the shaking direction, because the dilatancy of backfill was suppressed by the compression of backfill due to the bending deformation of backfill.

These trends of behaviour described above can be seen more in detail from Fig. 10, showing the behaviour of the

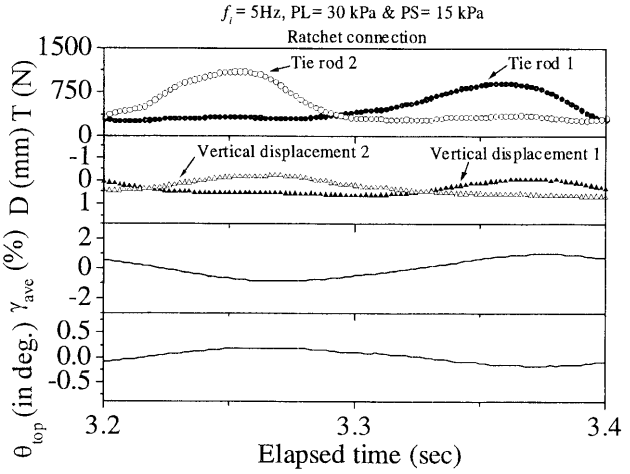


**Fig. 10. Detailed time histories of tie rod tension ($T$) and settlement ($D$) at the top platen, on each side of backfill, average shear strain ($\gamma_{ave}$) of backfill and rotation angle ($\theta_{top}$) at the top platen: model with a ratchet connection time $t = 3.2 - 3.4$ seconds (PL = 30 kPa and PS = 15 kPa at $f_i = 5$ Hz); elapsed**

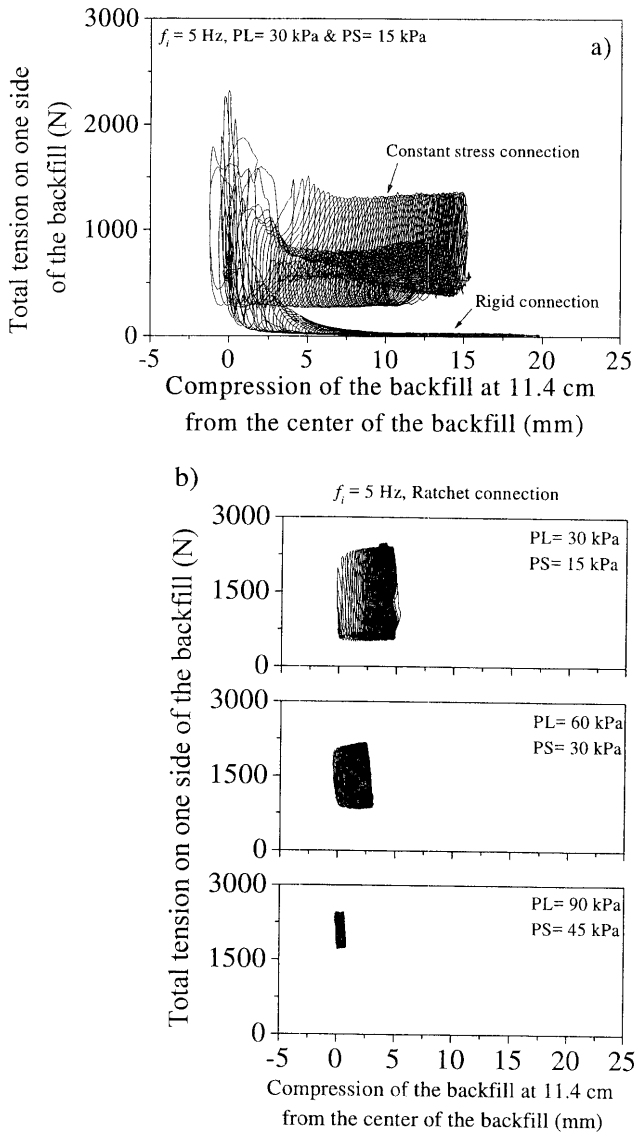


**Fig. 11. Relationships between total tie rod tension and compression of backfill on one side of backfill: a)two models with rigid and constant stress connections (PL = 30 kPa and PS = 15kPa;$f_i$ = 5Hz), and b) three tests with a ratchet connection (PL = 30 kPa and PS = 15 kPa, PL = 60 kPa and PS = 30 kPa, PL = 90 kPa and PS = 45 kPa; $f_i$ = 5 Hz)**

model with a ratchet connection for $t = 3.2$–$3.4$ seconds (note that the displacement D is positive for settlement at the crest of the model). That is, on the backside of the shaking direction, by the function of the ratchet connection, the increase in the height of backfill was very small accompanied by a large increase in the tie rod tension. On the front side of the shaking direction, on the other hand, the height of backfill was nearly constant with essentially no change in the tie rod tension. This behaviour was due to that the trend of dilatancy of backfill that was weak because of relatively small shear strains of backfill was balanced with the compression due to the bending deformation of backfill. In this figure, the function of a relatively soft spring which was activated when the height of backfill decreases in each single cycle of shaking is not apparent. However, this function was essential as the backfill exhibited noticeable residual compression in the course of shaking (*see* Fig. 7(b)).

Figure 11(a) and the top of Fig. 11(b) show the relationships between the total tension in the two tie rods and the settlement on one side of the backfill crest (at 11.4 cm from the center of the model) obtained from three tests on models with rigid, constant stress and ratchet connections (PL = 30 kPa and PS = 15 kPa). Figure 11(b) also shows similar results from two tests with a ratchet connection (PL = 60 kPa and PL = 90 kPa), which are explained later. The following trends of behaviour may be noted:

1) With a rigid connection, until the compression of backfill became about 5 mm, the lower bound of the tie rod tension decreased very rapidly with the compression of backfill (Fig. 11(a)). This behaviour was due to a relatively high stiffness of the tie rods. As the compression of backfill increased more, the tie rods loosened more, and the temporary increase in the tie rod tension by the increase in the backfill height became gradually smaller and finally became zero with no contribution of the tie rods to the stability of model.
2) With a constant stress connection, the average and amplitudes of tie rod tension were kept nearly constant throughout the shaking, irrespective of the compression of backfill (Fig. 11(a)).
3) With a ratchet connection, the amplitude and average of tie rod tension were also kept constant. However, these values were respectively larger and higher than those with a constant stress connection throughout the shaking, while the ultimate residual compression of backfill was much smaller (Fig. 11(b)).

Figures 12(a), (b) and (c) show the relationships between the average vertical stress measured at the central third of the bottom of the backfill by using a set of load

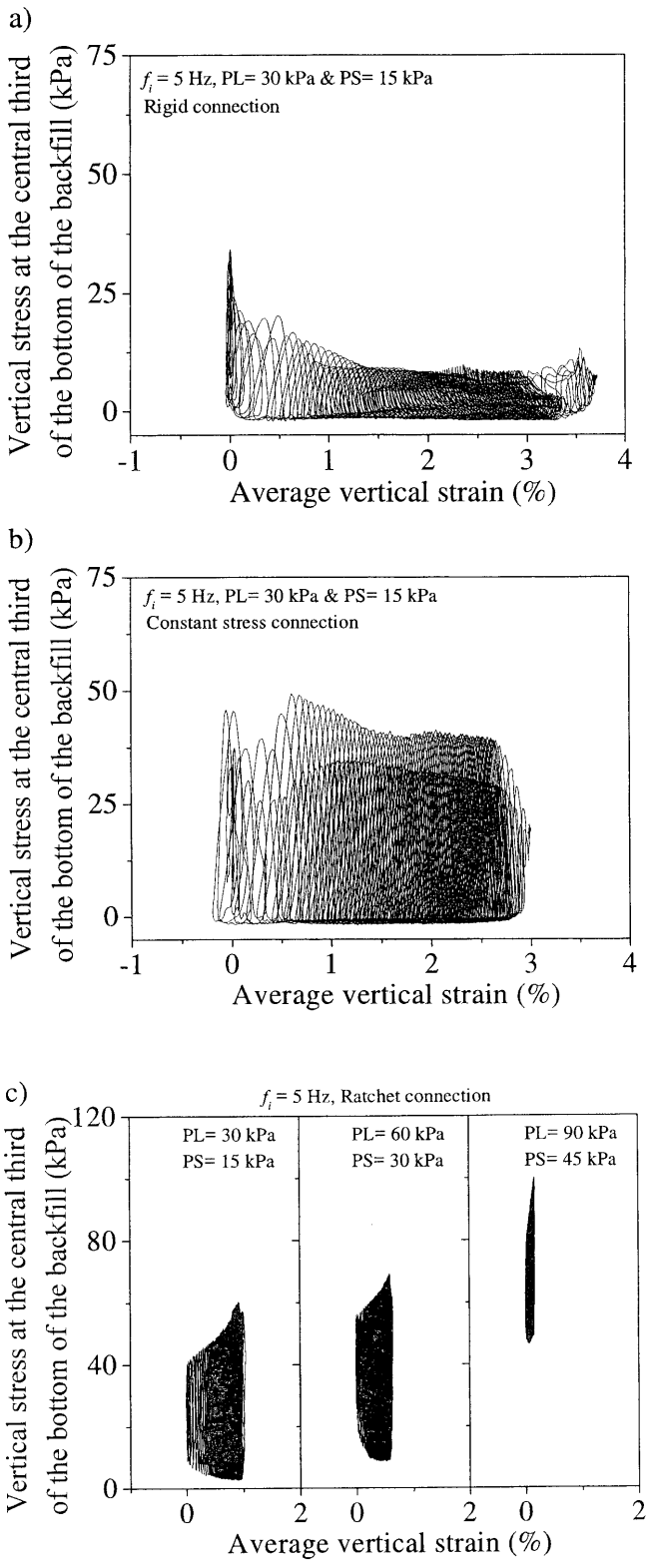


**Fig. 12. Relationships between vertical stress at the central third of the bottom of backfill and average vertical strain of backfill (PL = 30 kPa and PS = 15 kPa; $f_i$ = 5 Hz): a) model with a rigid connection, b) model with a constant stress connection, c) three tests with a ratchet connection (PL = 30 kPa and PS = 15 kPa, PL = 60 kPa and PS = 30 kPa, PL = 90 kPa and PS = 45 kPa; $f_i$ = 5 Hz)**

cells shown in Fig. 3(d) and the average vertical strain of backfill (positive in compression). With a rigid connection, the lower bound of the vertical stress dropped very fast with the compression of backfill, becoming essentially zero immediately after the compression of backfill started occurring (Fig. 12(a)). With a constant stress connection, although the average vertical stress was relatively high, the lower bound became temporarily essentially zero from a very early stage of shaking (Fig. 12(b)). With a ratchet connection, on the other hand, the lower bound of the vertical stress did not become zero at any moment during shaking (Fig. 12(c)). These results indicate that the use of a ratchet connection is essential to prevent the confining pressure in the backfill from becoming nearly zero during shaking. A gradual increase in the peak value of the vertical stress in the central zone at the bottom of the backfill during shaking when using a ratchet connection infers load transfer from the outer to the inner zones of backfill with progressive yielding in the outer zones.

Figures 13(a), (b) and (c) show the relationships between the average shear stress measured at the bottom of the backfill by using a set of load cells shown in Fig. 3(d) and the average shear strain of the backfill, which reflect the cyclic shear stress-shear strain behaviour in the backfill. The following trends of behaviour can be seen:

1) With a rigid connection (Fig. 13(a)), the behaviour was stiff only at the initial stage, where the input acceleration was increasing and the tie rod tension was still high. Subsequently, the backfill started softening largely due to; a) a large decrease in the vertical stress in the backfill (i.e., the prestress); b) a large increase in the shear stress by approaching a resonant state; and c) increased effects of strain-non-linearity on the stiffness of gravel associated with an increase in the shear strain (e.g., Tatsuoka et al., 1999a, b, c). As shown later, the natural frequency $f_n$ at the initial stage of the model, which was larger than the input frequency ($f_i$ = 5 Hz), decreased approaching $f_i$ during shaking. After having passed a transient resonant state, where $f_n \approx f_i$, the $f_n$ value became smaller than the $f_i$ value. Due to this non-stationary dynamic response of the model, the sign of the apparent peak-to-peak stiffness in each cycle in this figure changed from positive to negative ones. Note that the local peak-to-peak stiffness values in the backfill should not exhibit such a change in the sign as described above in the course of shaking. Three-dimensional dynamic response analysis will be necessary to fully understand this observed dynamic behaviour of the model.
2) A similar trend of behaviour, but in a more complicated manner, can be observed in the test using constant stress connection (Fig. 13(b)).
3) With a ratchet connection, the hysteretic loops were rather stationary showing only a small decrease in the average slope with an increase in the shear strain amplitude associated with an increase in the input acceleration (Fig. 13(c)). A moderate decrease in the apparent peak-to-peak stiffness was due primarily to

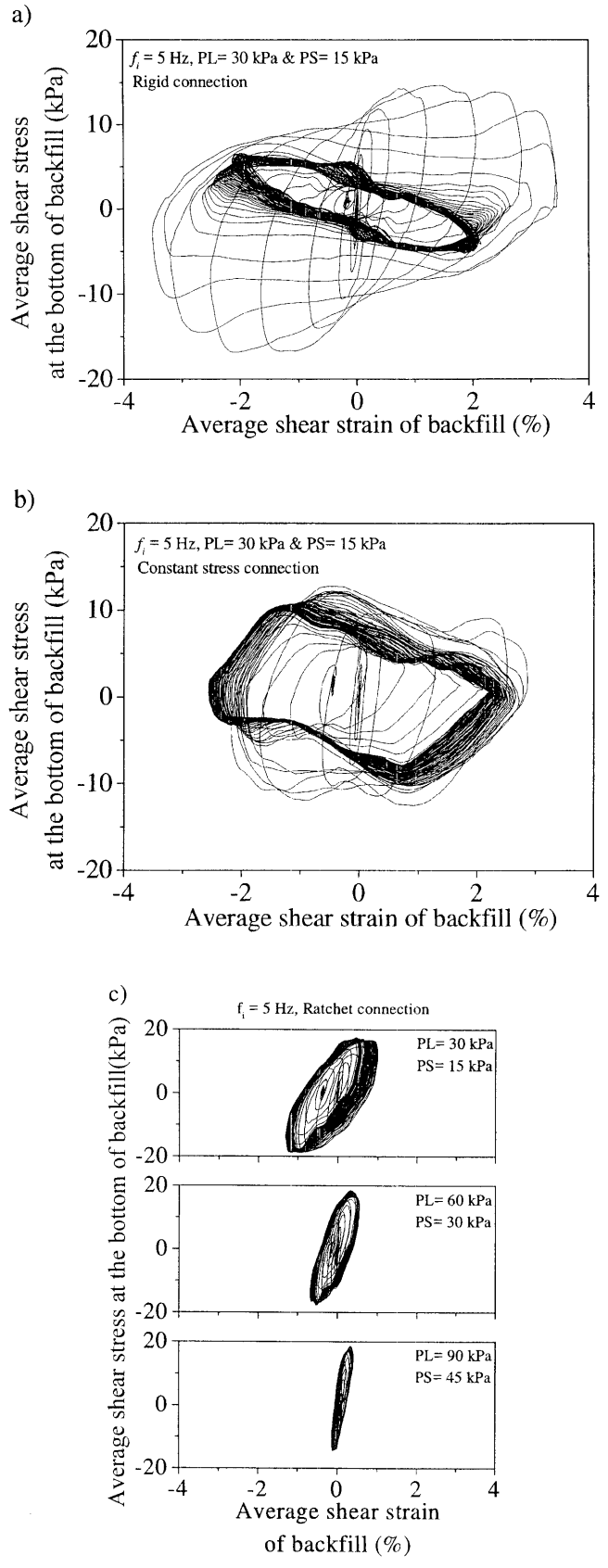


**Fig. 13. Relationships between average shear stress at the bottom of backfill and average shear strain of backfill (PL = 30 kPa and PS = 15 kPa; $f_i$ = 5 Hz): a) model with a rigid connection, b) model with a constant stress connection, c) three models with a ratchet connection (PL = 30 kPa and PS = 15 kPa, PL = 60 kPa and PS = 30 kPa, PL = 90 kPa and PS = 45 kPa; $f_i$ = 5 Hz)**

the effects of strain-non-linearity on the stress-strain property of gravel associated with an increase in the shear strain. It could also be seen that the resonant state was not reached in this test.

These test results shown above indicate that the deformation of PLPS reinforced soil structures subjected to very high seismic load could be kept very small by taking advantage of the two functions of the ratchet connection system, as illustrated in Fig. 5.

*Effects of Initial Prestress Level When Using a Ratchet Connection*

Three tests were performed on models having a ratchet connection at PS = 15 kPa, 30 kPa and 45 kPa with the preload level (PL) being twice the respective initial prestress (PS). The following trends of behaviour may be seen from the results of these tests (Fig. 14):

1) In all the three tests, the acceleration response was rather constant throughout the shaking (Fig. 14(a)), showing that the stress conditions in the backfill were essentially constant throughout each test because of using a ratchet connection.
2) The response acceleration at the crest of the model decreased with an increase in the initial PS level. This behaviour was due to the fact that the initial natural frequency ($f_n$) of the model, which was larger than the input frequency $f_i$ (= 5 Hz), became larger with an increase in the initial PS level, making the response state of the model more remote from the resonant state.
3) The residual compression of backfill significantly decreased with an increase in the initial PS level (Fig. 14(b)). This behaviour was due to a decrease in the shear strain in the backfill associated with an increase in the shear modulus of backfill induced by increasing the initial PS level (Fig. 14(d)).
4) The rotation at the top of the backfill was very small in all the three tests (Fig. 14(c)), but the effects of the initial PS level on this behaviour were not systematic. The reasons for the above are not known.
5) The peak and minimum levels of the average vertical stress at the top of the backfill were rather constant during each shaking test (Fig. 14(e)). Interestingly, the residual vertical stress at the end of shaking was slightly larger than the initial value in the two tests (PL = 30 kPa and PS = 15 kPa, PL = 90 kPa and PS = 45 kPa). This is due likely to the fact that part of the dilatancy of backfill caused by shear deformation remained at the end of shaking. This "locked" behaviour is indicative of the advantages of using a ratchet connection to fix the tie rods. The amplitude of vertical stress during shaking decreased with an increase in the initial PS level, which was due to a smaller response acceleration of the model at higher vertical stresses.

The trends of behaviour described above can be seen also from the behaviour presented in Figs. 8 and 9 and Figs. 11 through 13. In summary, to attain a higher seismic stability of PLPS reinforced soil structures, a higher

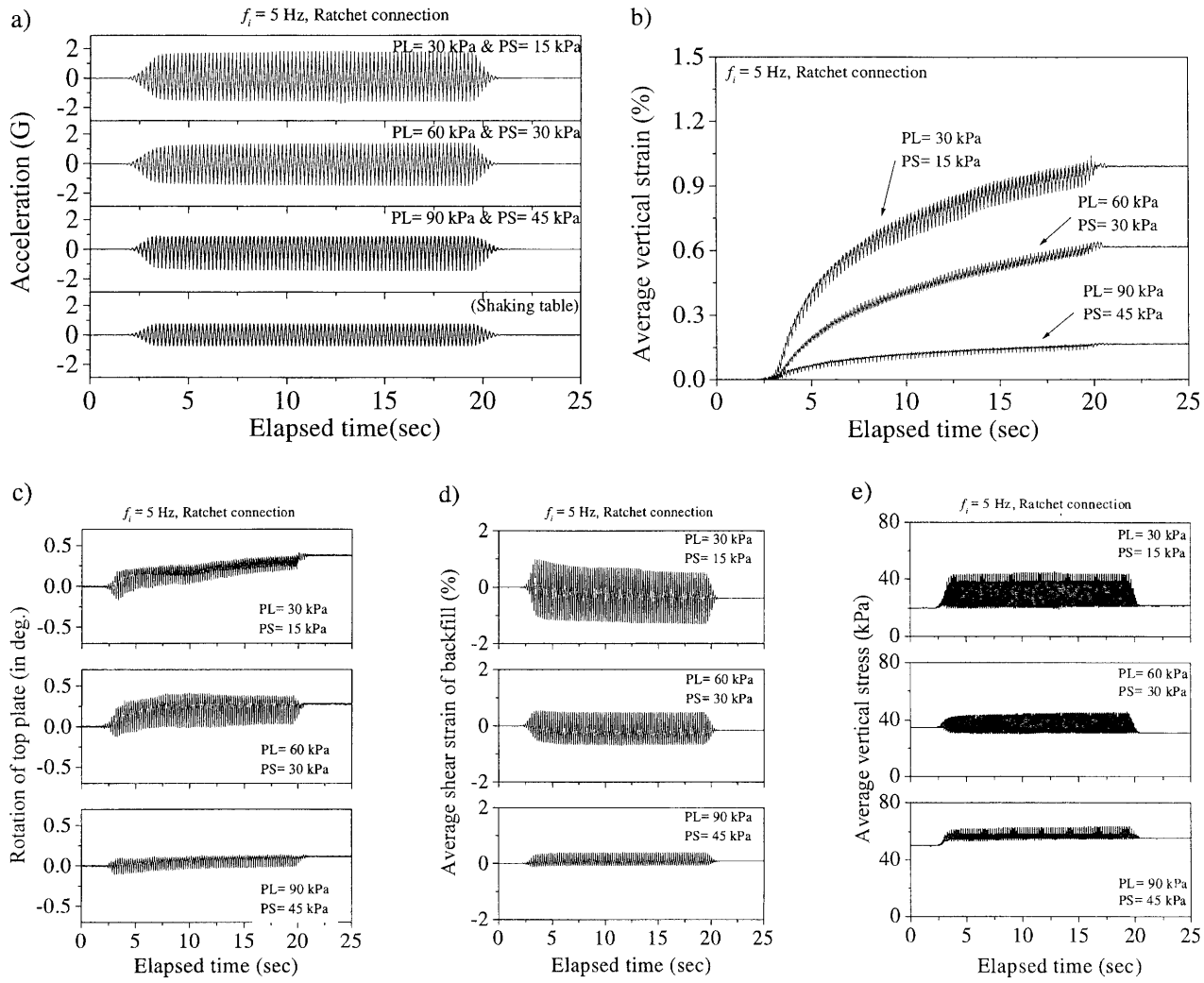


**Fig. 14. Time histories of: a) horizontal acceleration at the top platen (the top three) and the table (the bottom), b) average vertical strain of backfill, c) rotation of the top platen, d) average shear strain of backfill and e) average prestress, from three tests with the ratchet connection (PL = 30 kPa and PS = 15 kPa, PL = 60 kPa and PS = 30 kPa and PL = 90 kPa and PS = 45 kPa; $f_i$ = 5 Hz)**

initial PS level is preferable as long as the structure is not damaged during the preloading stage and the initial natural frequency of structure ($f_n$) is higher than the predominant frequency of design seismic load ($f_p$).

*Simplified Analysis of Dynamic Response Characteristics*

The dynamic response characteristics of the models observed in the present study are very complicated, mainly because they are not constant due to continuous changes in the stiffness of backfill caused by changes in the tie rod tension associated with shaking-induced changes in the height of backfill. For the first approximation, these characteristics were analysed in the framework of the theory for a single degree of freedom (SDOF). In this framework, the response ratio $L$ between the acceleration levels at the top and bottom of each model and the phase difference in $\varphi$ (in radian) between the top and bottom of each model are given as:

$$L = \sqrt{\frac{1+4\cdot h^2\cdot(f_i/f_n)^2}{\{1-(f_i/f_n)^2\}^2+4\cdot h^2\cdot(f_i/f_n)^2}} \tag{1a}$$

$$\tan\varphi = \frac{2\cdot h\cdot(f_i/f_n)^3}{1-(1-4h^2)\cdot(f_i/f_n)^2} \tag{1b}$$

where $h$ is the transient damping ratio of the model (unknown); $f_i$ is the given input frequency (= 5 or 10 Hz); and $f_n$ is the transient natural frequency of the model (unknown) (*see* Appendix C for more details). The theoretical relationships between $L$ and the frequency ratio $f_i/f_n$ and those between $\varphi$ and $f_i/f_n$ for different $h$ values are presented in Figs. 15(a) and (b) and other similar figures.

Transient values of $h$ and $f_i/f_n$ at representative moments during shaking of each model (as a SDOF system) were deduced by substituting measured values of $L$ and $\varphi$ into Eqs. 1(a) and 1(b) and iteratively solving these equations. The results of analysis for the three tests using different tie rods connection methods with PL = 30 kPa and PS = 15 kPa performed at $f_i$ = 5 Hz are presented in Figs. 15(a) and (b). Figure 15(c) shows the corresponding relationships between the measured single amplitude of

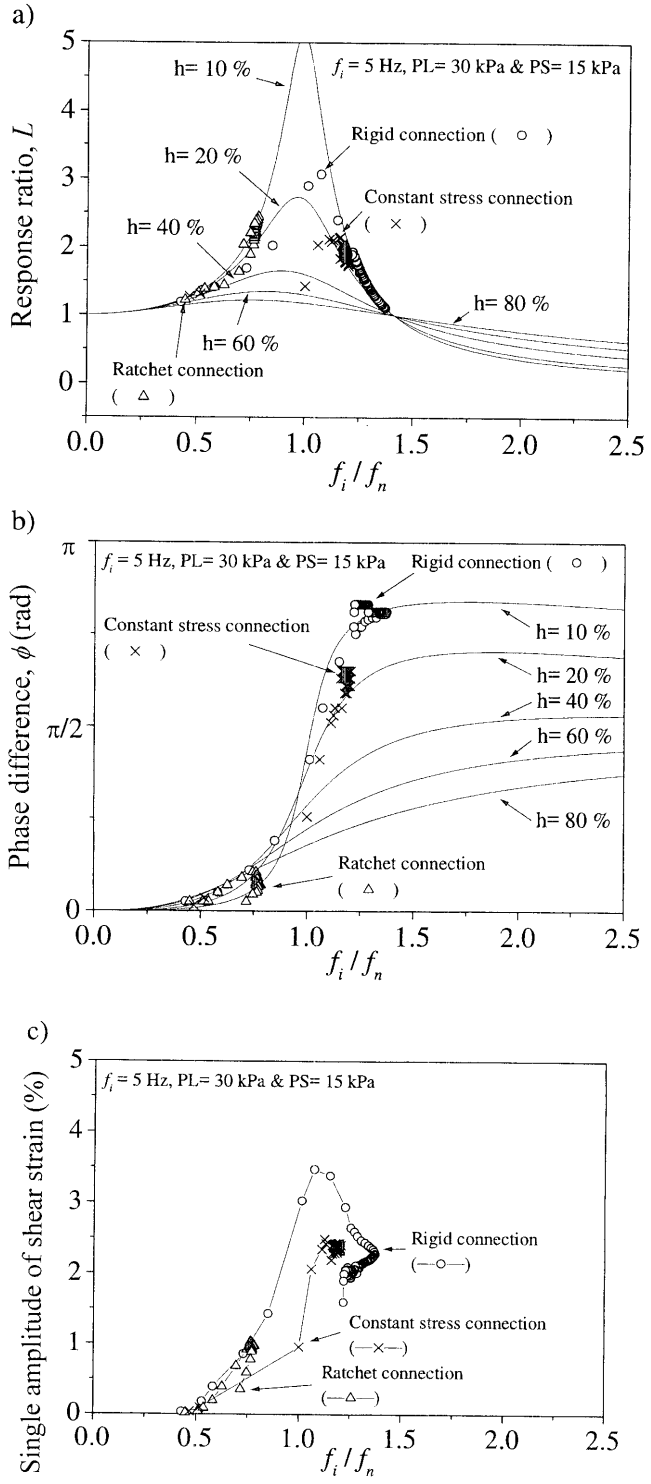


**Fig. 15. Relationships: a) between $L$ and $f_i/f_n$, and b) between $\varphi$ and $f_i/f_n$ for different $h$ values by the theory for a SDOF system and those from three tests with different connections of tie rod and c) experimental relationships between $\gamma_{sa}$ of the backfill and $f_i/f_n$ (PL = 30 kPa and PS = 15 kPa; $f_i$ = 5 Hz)**

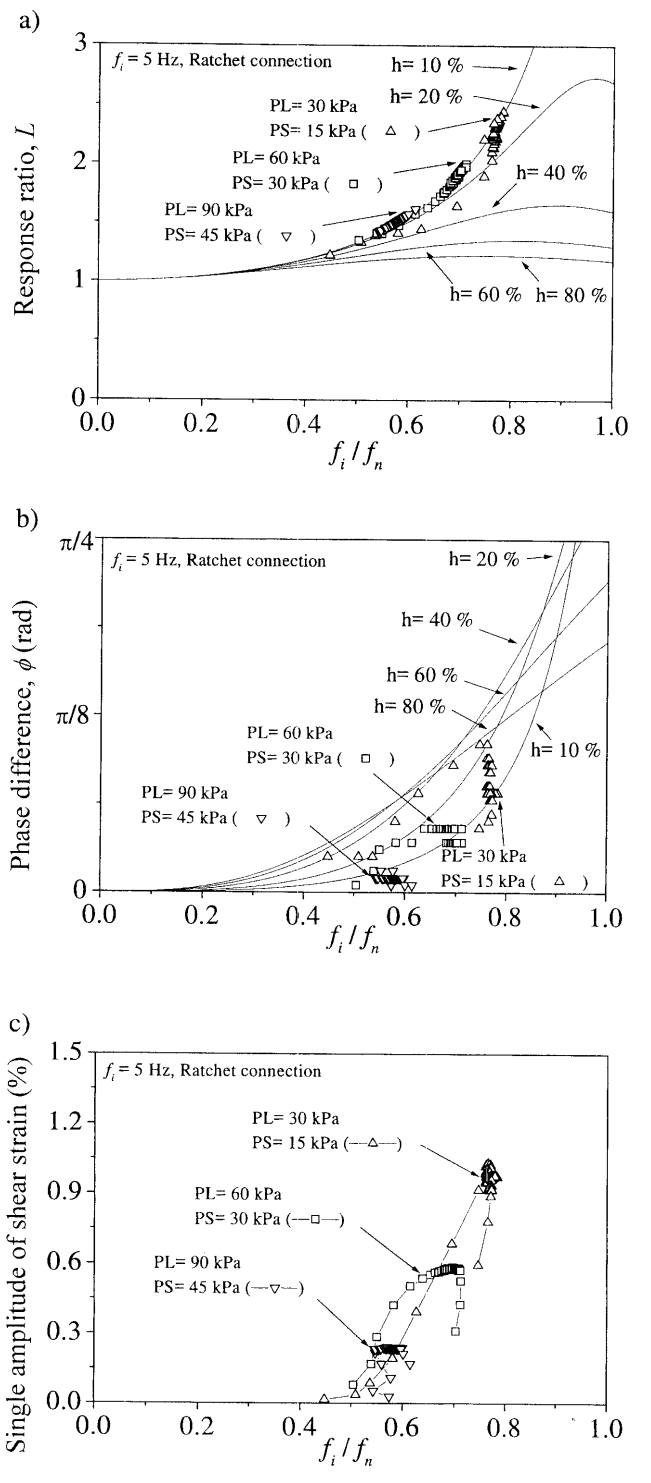


**Fig. 16. Relationships: a) between $L$ and $f_i/f_n$, b) between $\varphi$ and $f_i/f_n$ for different $h$ values by the theory for a SDOF system and those from three tests with a ratchet connection and different combinations of PL and PS kPa and c) experimental relationships between $\gamma_{sa}$ of backfill and $f_i/f_n$ ($f_i$ = 5 Hz)**

average shear strain $\gamma_{sa}$ of the backfill and the estimated value of $f_i/f_n$. The following trends of behaviour can be seen from these figures:

1) With rigid and constant stress connections, the value of $f_i/f_n$ increased from the respective initial value (lower than unity) towards a value larger than unity, passing a transient resonant state. In the two tests, the $\gamma_{sa}$ value became very large near and at the respective resonant state (Fig. 15(c)). As stated before, this large increase in the $f_i/f_n$ value when using a rigid connection was due to a significant decrease in the stiffness of the backfill caused: a) primarily by a sub-

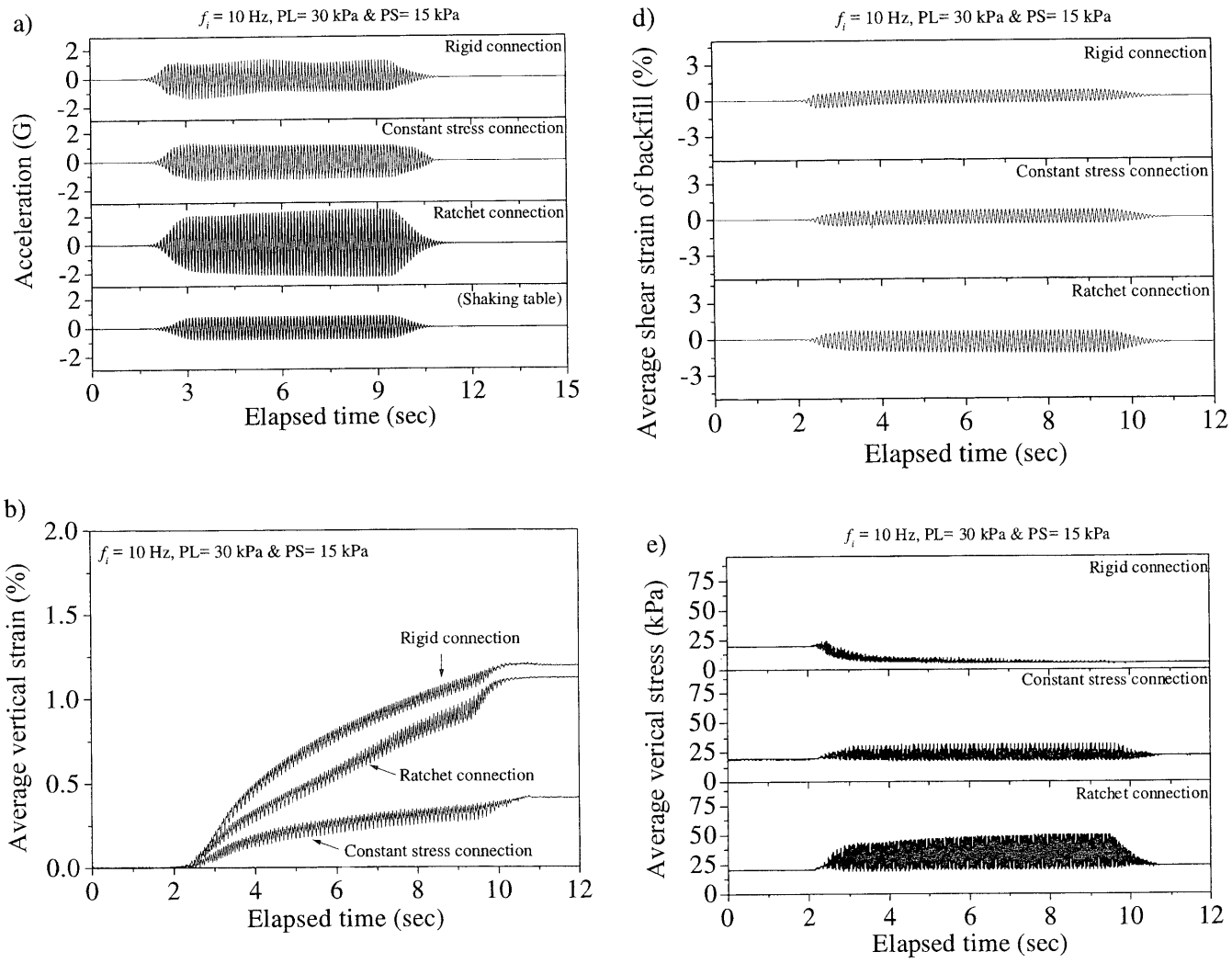


**Fig. 17. Time histories of: a) horizontal acceleration at the top platen (the top three) and the table (the bottom), b) average vertical strain of backfill, c) rotation of the top platen, d) average shear strain of backfill and e) average prestress from three tests with rigid, constant stress and ratchet connections (PL = 30 kPa and PS = 15 kPa; $f_i$ = 10 Hz)**

stantial decrease in the tie rod tension due to shaking-induced vertical residual compression of backfill; and b) partly by the non-linear stress-strain property of the gravel. With a constant stress connection, only the factor b) above was the major cause for the increases in the $f_i/f_n$ value. Therefore, the ultimate $f_i/f_n$ value when using a constant stress connection was lower than the value when using a rigid connection.

2) With a ratchet connection, the resonant state was not reached and the ratio $f_i/f_n$ was kept much lower than unity throughout the shaking. The value of $\gamma_{sa}$ was therefore kept much smaller than in the two other tests (Fig. 15(c)).

Figures 16(a), (b) and (c) compare the results from the three tests using a ratchet connection with three combinations of PL and PS levels, performed at $f_i$ = 5 Hz. It may be seen that with an increase in the initial PS, the response state was kept more remote from the respective resonant state with the largest values of $f_i/f_n$ and $\gamma_{sa}$ being kept smaller.

## TEST RESULTS ($f_i$ = 10 Hz)

To examine whether PLPS reinforced soil structures with a ratchet connection could be very stable even at a resonance, the same three types of the model described in

Fig. 7, having rigid, constant stress and ratchet connections with PL = 30 kPa and PS = 15 kPa, were shaken at $f_i$ = 10 Hz so that the resonant state could be reached. Figure 17 shows the results from these tests, while Figure 18 shows the summary of the analysis of the test results, similar to those presented in Figs. 15 and 16. The following trends of behaviour can be seen from these figures:

1) With a rigid connection, the average vertical stress at the top of the backfill decreased at a very high rate (Fig. 17(e)) as the backfill exhibited noticeable residual compression (Fig. 17(b)). Therefore, the natural frequency $f_n$ decreased very fast with cyclic loading. At an elapsed time of 2.3 seconds, the model exhibited the maximum ratio between the response acceleration at the top plate and the input acceleration at the shaking table (Fig. 17(a)), which indicates the existence of a transient resonant state as explained below. This behaviour enhanced a further increase in the residual compression of backfill and a further reduction in the vertical stress in the backfill. As the $f_n$ value decreased more, the response acceleration at the crest of the model and the shear deformation of backfill decreased noticeably, because the $f_i/f_n$ value became much larger than unity (Fig. 18). Despite the above, the bending deformation of backfill still continued increasing at the post-resonance state (Fig. 17(c)) due to a continuing reduction in the tie rod tension (Fig. 17(e)). As the resonance took place during the process where the input motion was increasing (Fig. 17(a)), the maximum values of the response acceleration at the crest of the model and the average shear strain of backfill were not the largest among the three tests.
2) With a ratchet connection, the lower bound of the average vertical stress at the top of the backfill did not become lower than the initial value throughout the shaking (Fig. 17(e)). On the other hand, the transient peak value of the average vertical stress became very large (Fig. 17(e)), because near-resonance vibration continued for nearly the whole period of shaking (Fig. 18). That is, at the resonant state, the response acceleration at the crest of the model exceeded two times the acceleration of gravity (i.e., 2 g) (Fig. 17(a)), which was the largest among the three tests. For this reason, the shear strain became the largest among the three tests (Fig. 17(d)) and the residual compression of backfill became relatively large, only slightly smaller than the value observed in the test using a rigid connection (Fig. 17(b)). Despite the above, the rotation of the top plate (i.e., the bending deformation of backfill) stayed very small throughout the test (Fig. 17(c)), which means that the model was not significantly damaged. It could also be seen from Fig. 18(b) that the damping ratio of the model (as a SDOF system) at the resonant state was as high as around 15% without exhibiting any serious structural damage. Usual reinforced concrete structures exhibit such a high damping value as above only when associated with serious structural damage.
3) The behaviour of the model with a constant stress connection was in between those of the other two. The smallest residual compression of backfill (Fig. 17(b)) was due to this intermediate behaviour

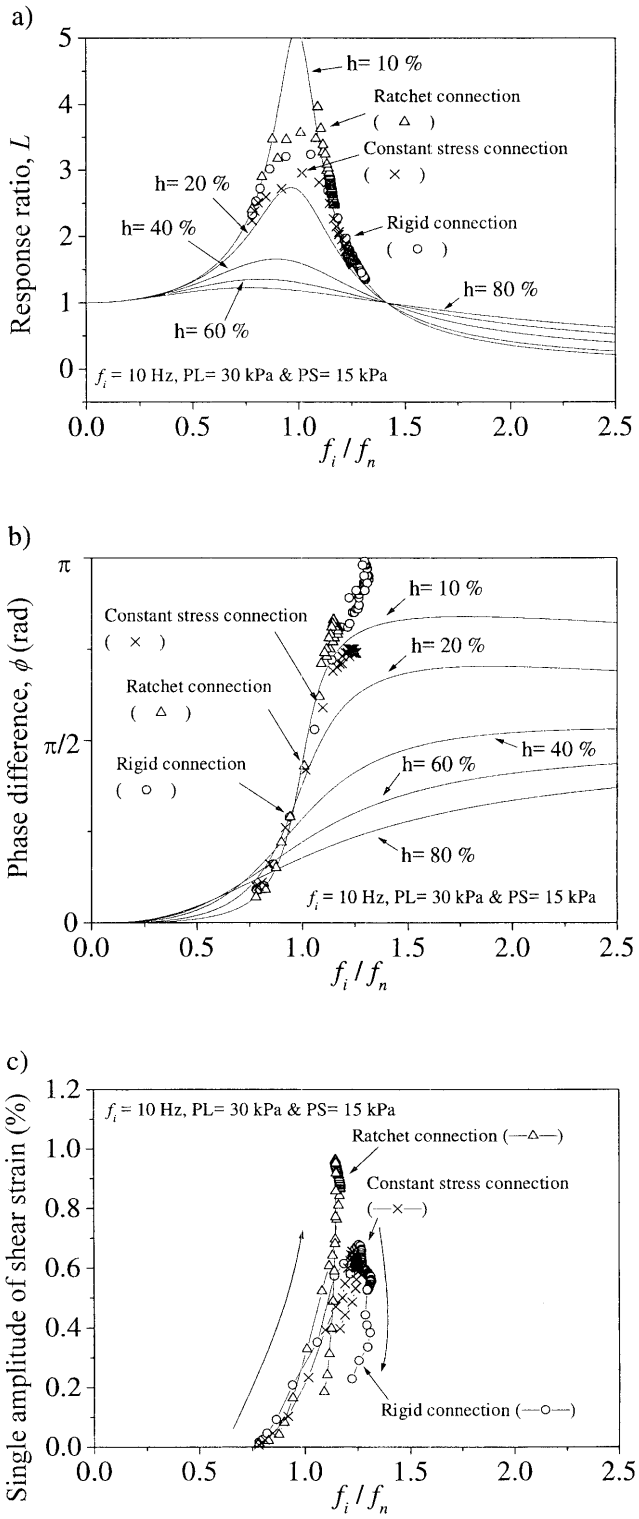


**Fig. 18. Relationships: a) between $L$ and $f_i/f_n$, b) between $\varphi$ and $f_i/f_n$ for different $h$ values by the theory for a SDOF system and those from three tests with different connections of tie rods and c) experimental relationships between $\gamma_{sa}$ of the backfill and $f_i/f_n$ (PL = 30 kPa and PS = 15 kPa; $f_i$ = 10 Hz)**

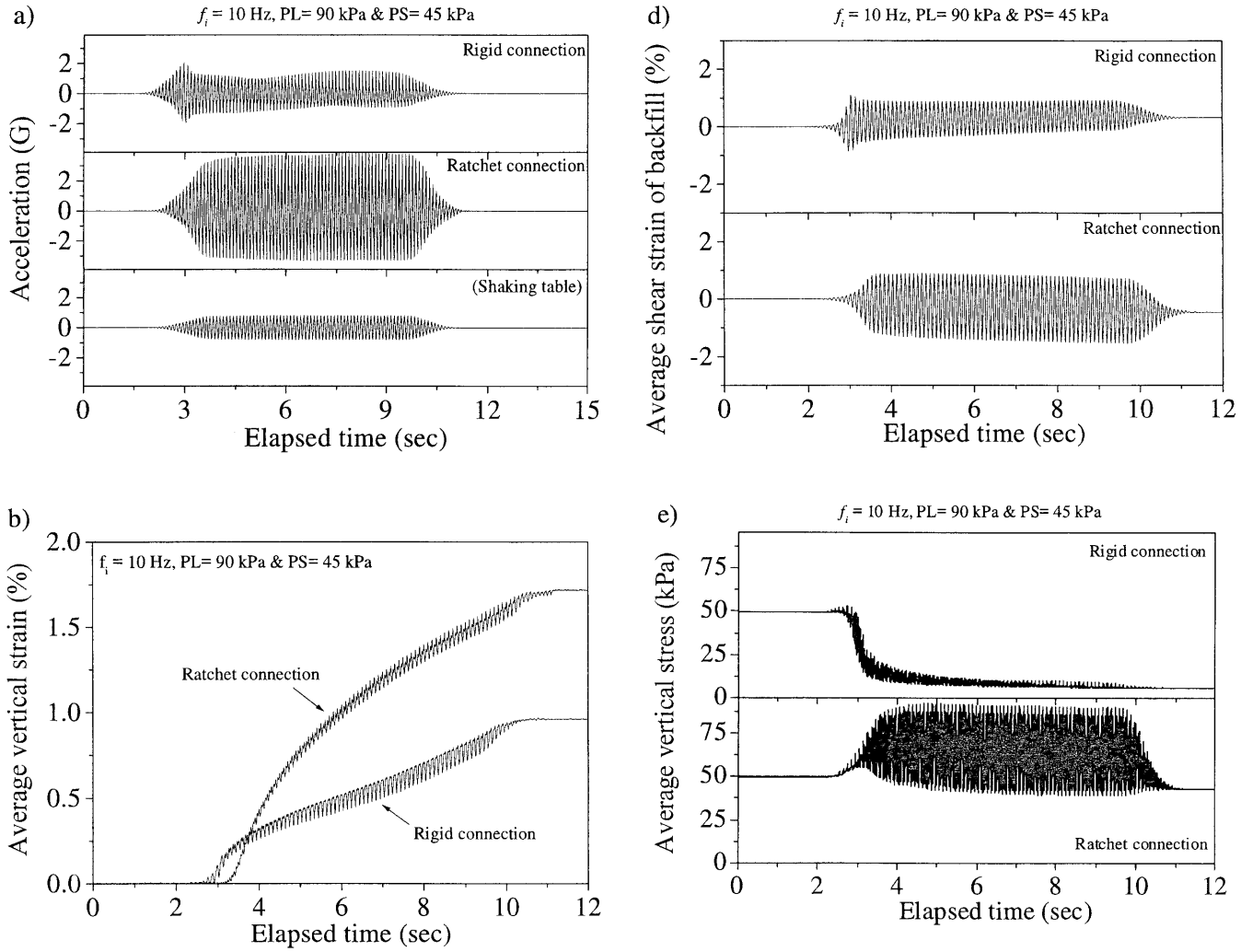


**Fig. 19. Time histories of: a) horizontal acceleration at the top platen (the top three) and the table (the bottom), b) average vertical strain of backfill, c) rotation of the top platen, d) average shear strain of backfill and e) average prestress from two tests with rigid and ratchet connections (PL = 90 kPa and PS = 45 kPa; $f_i$ = 10 Hz)**

(i.e., larger average vertical stress at the top of backfill than in the test using a rigid connection, but a smaller response acceleration than in the test using a ratchet connection).

Figures 19 and 20 show results from two similar tests with rigid and ratchet connections performed at $f_i$ = 10 Hz, but with PL = 90 kPa and PS = 45 kPa. Similar trends of behaviour as described above can be seen more clearly. On the other hand, by comparing respectively Figs. 17(a) and 19(a), Figs. 18(a) and 20(a) and Figs. 18(c) and 20(c), it may be seen that when using a ratchet connection, as the initial PS level became larger from 15 kPa to 45 kPa, the response acceleration at the crest of the model near to and at the resonant state became larger, exceeding 3.5 g (Fig. 19(a)). The average shear strain of backfill became larger corresponding by. Analysis of the test results (Figs. 18(a) and 20(a)) suggests that this trend of behaviour was due to a decrease in the damping value near to and at the resonant state with the increase in the initial PS level from 15 kPa to 45 kPa. Smaller damping values of the model using a ratchet connection with the initial PS = 45 kPa may reflect smaller structural damage to the model, as deduced from a very small rotation at the top plate (Fig. 19(c)).

## ESTIMATION OF THE NATURAL FREQUENCY OF STRUCTURE

It is necessary to evaluate in a rational manner the ini-

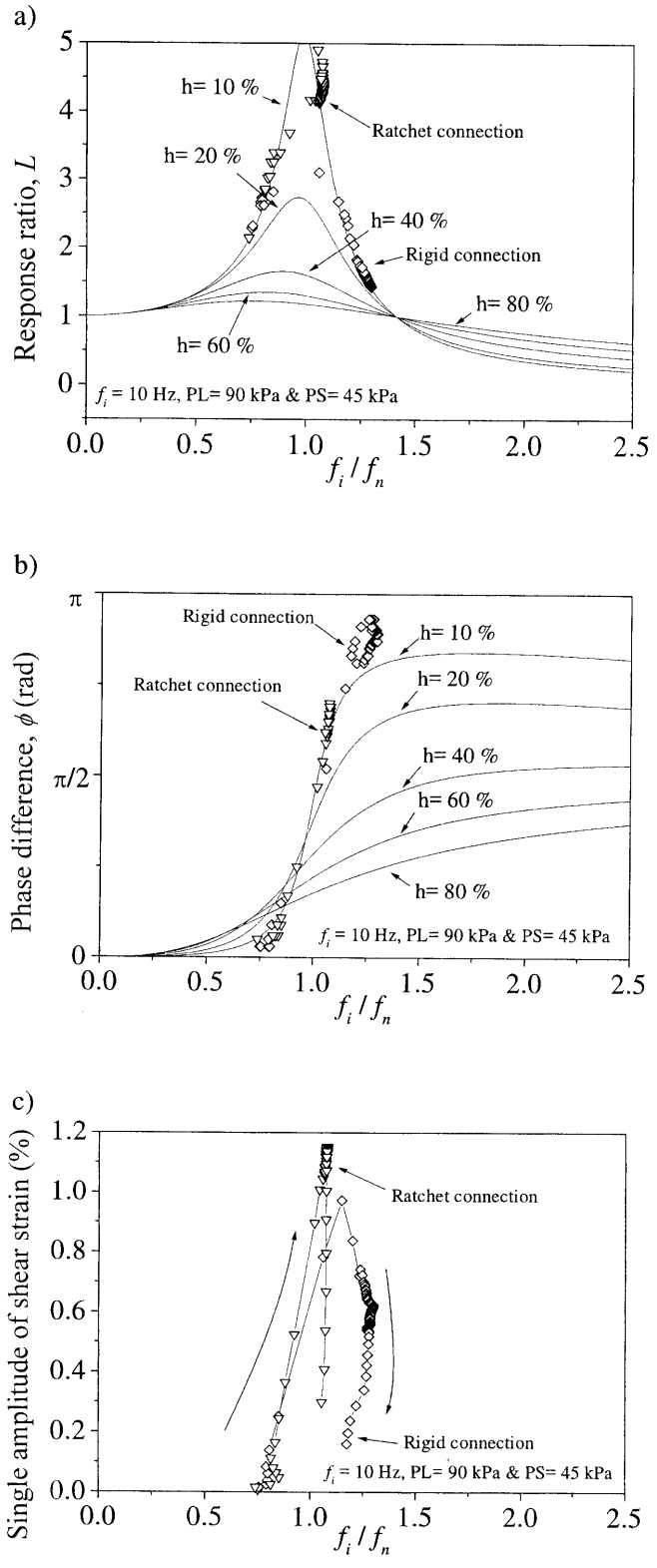


**Fig. 20. Relationships: a) between $L$ and $f_i/f_n$, b) between $\varphi$ and $f_i/f_n$ for different $h$ values by the theory for a SDOF system and those from two tests with rigid and ratchet connections and c) experimental relationships between $\gamma_{sa}$ of the backfill and $f_i/f_n$ (PL = 90 kPa and PS = 45 kPa; $f_i$ = 10 Hz)**

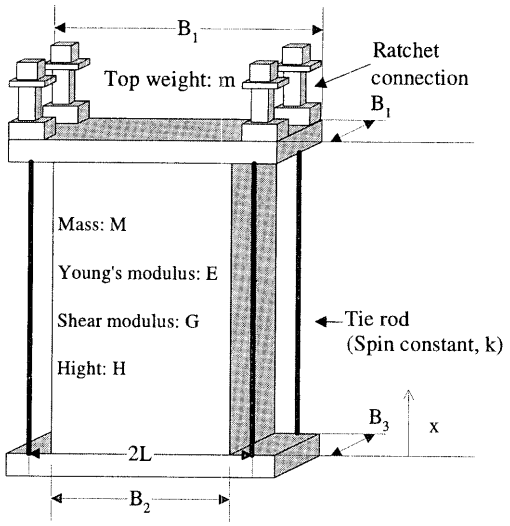


**Fig. 21. Model configurations to obtain the natural frequency of a model with a ratchet connection**

tial value of the natural frequency $f_n$ and those during shaking of a given PLPS GRS structure so that the occurrence of resonance for a given design seismic load can be avoided by adjusting the initial $f_n$ value of the structure. To that end, a simplified method to estimate the initial $f_n$ value of a given PLPS mechanically reinforced backfill structure was developed based on the following assumptions:

1) The backfill is a uniform isotropic linear elastic material having given Young's modulus $E$ and shear modulus $G$. The total mass is $M$ and the height of the backfill is $H$ (Fig. 21).
2) The deformation of backfill consists of bending and shearing modes as a simple beam.
3) The top plate does not rotate, being fully fixed by tie rods.

The last assumption is relevant to the models with a ratchet connection and to the models with a rigid connection when the tie rod tension is kept high enough. As this assumption is not relevant to models with a constant stress connection, the behaviour of this type of model is not analysed below.

From the condition that the maximum kinetic energy is equal to the maximum strain energy, an equation can be derived that gives the transient natural frequency $f_n$ of a given model with known quantities of the parameters shown in Fig. 21 (*see* Appendix C for details). Figure 22 shows the theoretical relationships between the natural frequency $f_n$ of model and the shear modulus $G$ of backfill, obtained by the method described above, for the models with rigid and ratchet connections for a range of $f_n$ relevant to these two models. A slight difference between the two curves is due to the weight of the ratchet connection system. Effects of PL and initial PS levels and the frequency of input motion on these relationships appear through the effects of these factors on the Young's modulus $E$ and shear modulus $G$. In addition, as the stiffness of backfill is a function of instantaneous vertical

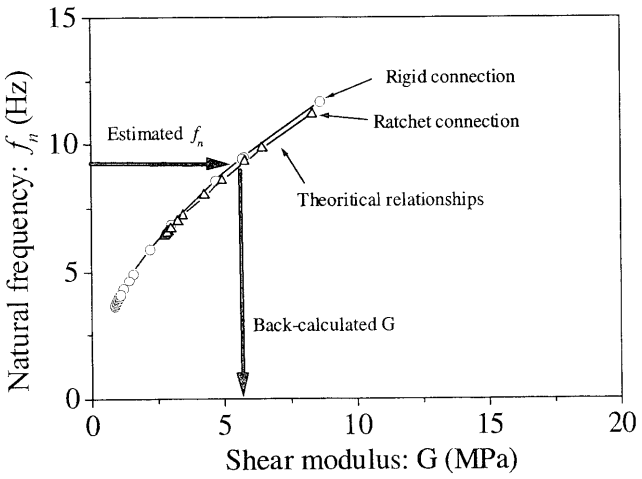


Fig. 22. Theoretical relationships between $f_n$ and shear modulus $G$ of backfill for models with rigid and ratchet connections

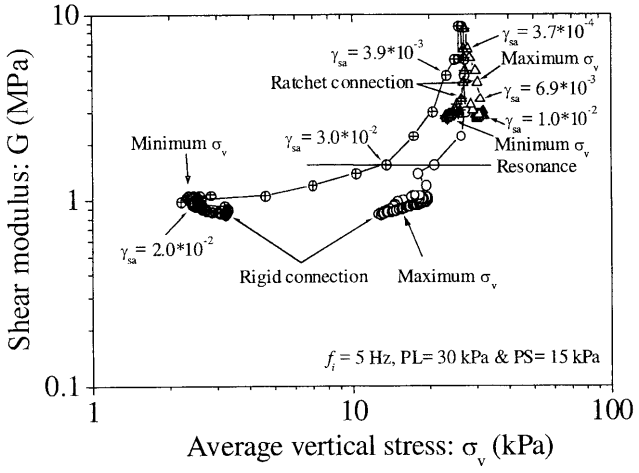


Fig. 23. Relationships between back-calculated shear modulus $G$ of backfill and measured vertical stress $\sigma_v$ at the bottom of backfill in the model with a rigid connection and a ratchet connection (PL = 30 kPa and PS = 15 kPa; $f_i$ = 5 Hz).

stress and strain in the backfill and loading history, it changes during shaking. As illustrated in Fig. 22, the instantaneous $G$ value of backfill at each moment during shaking was back calculated by substituting the respective instantaneous value of $f_n$ that was deduced based on Eqs. 1(a) and 1(b) for each model as a SDOF system. Due to a limited amount of available publication space, only analysis of the results from the tests at $f_i$ = 5 Hz is presented below.

Figure 23 shows the relationships between the back-calculated $G$ value of backfill and the corresponding measured average vertical stress ($\sigma_v$) at the top of backfill for the two tests (PL = 30 kPa and PS = 15 kPa at $f_i$ = 5 Hz) described in Fig. 7. The average shear modulus $G$ in each cycle is plotted against the maximum and minimum values of $\sigma_v$ in that cycle that were measured with load cells equipped at the bottom of the backfill. The single amplitudes of the average shear strain $\gamma_{sa}$ of backfill at several representative moments are also indicated. Figure 24 shows the corresponding relationships between the deduced $G$ value and the measured value of $\gamma_{sa}$. The values of the maximum and minimum values of $\sigma_v$ in the backfill at several representative moments are indicated in these figures. The values of shear stress $\tau$ obtained as $\tau = G^*\gamma_{sa}$ are also indicated in Fig. 24. The following trends of behaviour can be seen from these figures:

1) With a rigid connection, the decrease in the shear modulus $G$ of backfill with the increase in $\gamma_{sa}$ was enhanced by a substantial decrease in the vertical stress $\sigma_v$ and the development of large shear stresses $\tau$ as a result of resonance. The shear modulus $G$ after the resonance was considerably smaller than the value for the same $\gamma_{sa}$ value before the resonance (Fig. 24).

   This would be due to a large drop in the $\sigma_v$ value (Fig. 23) and structural damage to the backfill by large shear strains experienced near to and at the resonant state.

2) With a ratchet connection, the rate of the decrease in the $G$ value with an increase in $\gamma_{sa}$ was lower due to higher values of $\sigma_v$ (Fig. 23) and smaller shear stresses $\tau$ (because of non-occurrence of a resonance) (Fig. 24). The difference in the $G$ values at the same $\gamma_{sa}$ when $\gamma_{sa}$ was increasing and decreasing was noticeably smaller than the value with a rigid connection (Fig. 24). This behaviour was due likely to smaller structural damage to the backfill with a ratchet connection.

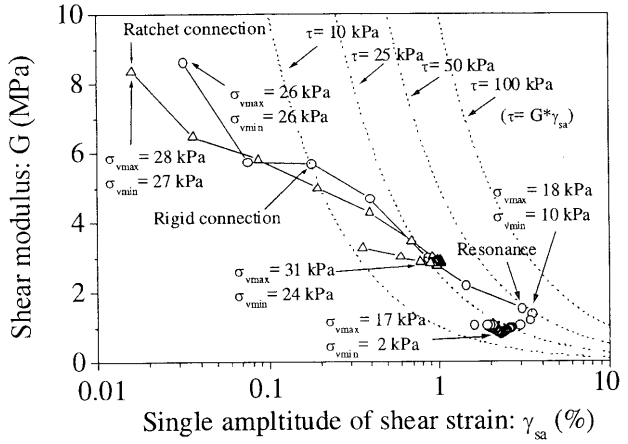


Fig. 24. Relationships between back-calculated shear modulus $G$ and measured shear strain $\gamma_{sa}$ of backfill in the model with a rigid connection and a ratchet connection (PL = 30 kPa and PS = 15 kPa; $f_i$ = 5 Hz)

These data show again the advantages of using a ratchet connection.

A theoretical relationship between the natural frequency $f_n$ of structure and the shear modulus $G$ of backfill for given structural configurations, as presented in Fig. 22, can be obtained by following the method described in this paper. The value of $G$ of backfill as a function of instantaneous strain and confining pressure can be obtained from relevant laboratory stress-strain tests on the backfill material. The initial value of $f_n$ can be esti-

mated in a rather straightforward way, as the initial value of $G$ of backfill at strains of the order of 0.01% can be estimated for a given initial prestress level. On the other hand, the estimate of the values of $f_n$ during shaking for given structural and dynamic loading conditions is much more complicated. However, the experimental data presented in this paper suggest that the resonant state can be avoided by using a ratchet connection and setting the initial value of $f_i$ sufficiently higher than the anticipated predominant frequency $f_p$ of a given seismic load.

## CONCLUSIONS

The following conclusions can be derived from the test results presented in this paper:

1) The shear and bending deformation and associated residual compression of mechanically reinforced backfill structures subjected to high dynamic load can be substantially reduced by maintaining the vertical stress in the backfill sufficiently high during dynamic loading to keep the stiffness and strength of backfill sufficiently high, when compared with cases where the vertical stress is allowed to decrease largely.
2) To the end described above, it is effective to use a ratchet connection, having the following two function, to fix the tie rods used to preload and prestress the backfill:
   a) The vertical stress in the backfill is kept nearly constant when the backfill height tends to decrease (i.e., the constant pressure condition of the backfill).
   b) The height of backfill is kept nearly constant when the backfill height tends to increase (i.e., the constant height condition of the backfill).
3) Therefore, by setting the initial natural frequency of structure sufficiently higher than the predicted predominant frequency of given design dynamic load, the possibility of approaching the resonant state can become very small by using a ratchet connection.
4) By the two functions a) and b) listed above, mechanically reinforced backfill structures with a ratchet connection would not be seriously damaged even if extremely high-level dynamic load is applied by approaching the resonant state. Relatively high damping values could be exhibited by such soil structures without serious structural damage.
5) To attain smaller deformation of mechanically reinforced backfill structures subjected to high dynamic load, a higher prestress is preferable as long as the structure is not damaged during the preloading and prestressing stage and the initial natural frequency of the structure is kept sufficiently higher than the predominant frequency of given design dynamic load.

## ACKNOWLEDGEMENTS

The authors are sincerely grateful to cooperation provided by Messrs. Sugimura, Y. at Ministry of Transport (formerly graduate student, University of Tokyo), Kikuchi, T. at Kajima Corporation (formerly undergraduate student, University of Tokyo), Ishimura, T. at University of Tokyo, Nakamura, S. at Science University of Tokyo, Yamamoto, S. at Yamagi Construction Co., Ltd. (formerly undergraduate student, Science University of Tokyo), Natsuki, T. at Araigumi Co., Ltd. in performing the present study at the University of Tokyo. The authors sincerely acknowledge a critical review of the manuscript by Prof. Leshchinsky, D., the University of Delaware.

## REFERENCES

1) Bathurst, R. J. and Alfaro, M. C. (1997): Review of seismic design, analysis and performance of geosynthetic reinforced walls, slopes and embankments, *Earth Reinforcement* (eds. by Ochiai et al.), Balkema, **II**, 887–918.
2) Bathurst, R. J. and Hatami, K. (1998): Seismic response analysis of a geosynthetic-reinforced soil retaining wall *Geosynthetic Int.*, **5** (1-2) 127–166.
3) Hatami, K. and Bathurst, R. J. (2001): Investigation of seismic response of reinforced soil retaining walls, *CD-ROM Proc. of Fourth Int. Conf. on Recent Advances in Geotech. Earthquake Engrg. and Soil Dynamics and Symp. in Honor of Prof.* W. D. Liam Finn, (7,18).
4) Iwasaki, T., Tatsuoka, F. and Takagi, Y. (1978): Shear moduli of sands under cyclic torsional loading, *Soils and Foundations*, **18** (1), 39–56.
5) Japanese Geotechnical Society (1996): Special issue on the geotechnical aspects of the January 1995 Hyogoken-Nambu Earthquake, *Soils and Foundations*, Special Issue for the 1995 Hyogoken-Nambu Earthquake.
6) Kikuchi, T., Sugimura, Y., Shinoda, M., Tatsuoka, F. and Uchimura, T. (1999): Laboratory cyclic loading tests on preloaded prestressed reinforced soil structure models, *Proc. of the 34th Japan National Conf. on Geotech. Engrg,* **2**, 1781–1782 (in Japanese).
7) Koseki, J., Munaf, Y., Tatsuoka, F., Tateyama, M. and Kojima, K. (1998): Shaking table and tilting tests of geosynthetic-reinforced soil retaining wall and conventional type retaining wall models, *Geosynthetics Int.*, **5** (1-2), 73–96.
8) Murata, O., Tateyama, M. and Tatsuoka, F. (1994): Shaking table tests on a large geosynthetic-reinforced soil retaining wall model, *Proc. of Int. Symp. Recent Case Histories of Permanent Geosynthetic-Reinforced Soil Retaining Walls* (eds. by Tatsuoka and Leshchinsky), Balkema, 259–264.
9) Nakarai, K., Shinoda, M., Yamamoto, S., Koima, K., Tateyama, M., Uchimura, T. and Tatsuoka, F. (2000): Natural frequency of full-scale preloaded and prestressed geosynthetic-reinforced soil pier, *Geosynthetics Engrg. J.*, IGS Japan Chapter, 302–311 (in Japanese).
10) Peng, F. L., Kotake, N., Tatsuoka, F., Hirakawa, D. and Tanaka, T. (2000): Plane strain compression behaviour of geogrid-reinforced sand and its numerical analysis, *Soils and Foundations*, **40** (3), 55–74.
11) Rocha, M. (1957): The possibility of solving soil mechanics problems by the use of models, *Proc. of the 4th Int. Conf. on Soil Mechanics*, **1**, 183–188.
12) Shinoda, M., Uchimura, T., Maruyama, N. and Tatsuoka, F. (1999): Effects of preloading and prestressing on the vertical stiffness of GRS structure, *Proc. of the 11th ARC on Soil Mechanics and Geothech. Engrg.*, **1**, 419–422.
13) Shinoda, M., Uchimura, T., Tatsuoka, F. and Tateyama, M.

(2000a): Seismic stability of preloaded and prestressed reinforced soil structures, *Proc. of the 2nd Asian Geosynthetics Conf.*, **2**, 43–48.
14) Shinoda, M., Uchimura, T., Sugimura, Y., Tatsuoka, F. and Tateyama, M. (2000b): High seismic performance of preloaded and prestressed geotextile-reinforced soil structures, *CD-ROM Proc. of an Int. Conf. on Geotech. and Geological Engrg.*, GIGS0447.PDF.
15) Shinoda, M., Uchimura, T. and Tatsuoka, F. (2001a): Increasing the stiffness of mechanically reinforced backfill by preloading and prestressing, *Soils and Foundations*, **43** (1), 75–92.
16) Shinoda, M., Uchimura, T., Tatsuoka, F., Tateyama, M. and Natsuki, T. (2001b): A new simple method to substantially increase the seismic stability of reinforced soil structures, *J. of Soil Dynamics and Earthquake Engrg.* **22** (9–12), 1115–1123.
17) Tatsuoka, F., Tateyama, M. and Koseki, J. (1996): Performance of soil retaining walls for railway embankments, *Soils and Foundations*, Special Issue for the 1995 Hyogoken-Nambu Earthquake, 311–324.
18) Tatsuoka, F., Uchimura, T. and Tateyama, M. (1997a): Preloaded and prestressed reinforced soil, *Soils and Foundations*, **37** (3), 79–94.
19) Tatsuoka, F., Tateyama, M., Uchimura, T. and Koseki, J. (1997b): Geosynthetic-reinforced soil retaining walls as important permanent structures, 1996–1997 Mercer Lecture, *Geosynthetic Int.*, **4** (2), 81–136.
20) Tatsuoka, F., Koseki, J. and Tateyama, M. (1997c): Performance of reinforced soil structures during the 1995 Hyogoken-Nambu Earthquake, Special Lecture, *Int. Symp. on Earth Reinforcement (IS Kyushu '96)*, Balkema, **2**, 973–1008.
21) Tatsuoka, F., Koseki, J., Tateyama, M., Munaf, Y. and Horii, N. (1998): Seismic stability against high seismic loads of geosynthetic-reinforced soil retaining structures, Keynote Lecture, *Proc. 6th Int. Conf. on Geosynthetics*, Atlanta, **1**, 103–142.
22) Tatsuoka, F., Jardine, R. J., Lo Presti, D., Di Benedetto, H. and Kodaka, T. (1999a): Characterising the pre-failure deformation properties of geomaterials, Theme Lecture for the Plenary Session No.1, *Proc. of XIV IC on SMFE, Hamburg*, September 1997, **4**, 2129–2164.
23) Tatsuoka, F., Modoni, G., Jiang, G. L., Anh Dan, L. Q., Flora, A., Matsushita, M. and Koseki, J. (1999b): Stress-strain behaviour at small strains of unbound granular materials and its laboratory Tests, Keynote Lecture, *Proc. of Workshop on Modelling and Advanced Testing for Unbound Granular Materials, January 21 and 22, 1999, Lisboa* (ed. by Correia), Balkema, 17–61.
24) Tatsuoka, F., Correia, A. G., Ishihara, M. and Uchimura, T. (1999c): Non-linear resilient behaviour of unbound granular materials predicted by the cross-anisotropic hypo-quasi-elasticity model, *Proc. of Workshop on Modelling and Advanced Testing for Unbound Granular Materials, January 21 and 22, 1999, Lisboa* (ed. by Correia), Balkema, 197–204.
25) Tatsuoka, F., Santucci de Magistris, F., Hayano, K., Momoya, Y. and Koseki, J. (2000): Some new aspects of time effects on the stress-strain behaviour of stiff geomaterials, Keynote Lecture, *The Geotechnics of Hard Soils-Soft Rocks, Proc. of Second Int. Conf. on Hard Soils and Soft Rocks, Napoli, 1998* (eds. by Evamgelista and Picarelli), Balkema **2**, 1285–1371.
26) Tatsuoka, F., Uchimura, T., Hayano, K., Di Benedetto, H., Koseki, J. and Siddiquee, M. S. A. (2001a): Time-dependent deformation characteristics of stiff geomaterials in engineering practice, the Theme Lecture, *Proc. of the Second Int. Conf. on Pre-Failure Deformation Characteristics of Geomaterials, Torino, 1999*, Balkema (eds. by Jamiolkowski et al.), 2, 1161–1262.
27) Tatsuoka, F., Ishihara, M., Di Benedetto, H. and Kuwano, R., (2001b): Time-dependent shear deformation characteristics of geomaterials and their simulation, *Soils and Foundations*, **42** (2), 103–129.
28) Tatsuoka, F., Masuda, T. and Siddiquee, M. S. A. (2001c): Modelling the stress-strain behaviour of sand in cyclic plane strain loading, *Soils and Foundations*, **42** (2), 1–22.
29) Uchimura, T., Tatsuoka, F., Sato, T., Tateyama, M. and Tamura, Y. (1996): Performance of preloaded and prestressed geosynthetic-reinforced soil, *Proc. Int. Symp. Earth Reinforcement, Fukuoka* (eds. by Ochiai et al.), Balkema, **1**, 537–542.
30) Uchimura. T., Tatsuoka, F, Tateyama, M. and Koga, T. (1998): Preloaded-prestressed geogrid-reinforced soil bridge pier, *Proc. 6th Int. Conf. on Geosynthetics*, Atlanta, **2**, 565–572.
31) Uchimura, T., Shinoda, M., Tatsuoka, F. and Tateyama, M. (2001): Performance of PLPS geosynthetic-reinforced soil structure against working and seismic loads, *Proc. of the 15th Int. Conf. on Soil Mechanics and Geotech. Engrg., Istanbul,* **2**, 1633–1636.
32) Uchimura, T., Tatsuoka, F., Shinoda, M., Sugimura, Y. and Kikuchi, T. (2002): Roles of tie rods for seismic stability of preloaded and prestressed reinforced soil structures, *Proc. of the 7th Int. Conf. on Geosynthetics*, Nice, **1** 115–118 .
33) White, D. M. and Holtz, R. D. (1996): Performance of geosynthetic-reinforced slopes and walls during the northridge, California Earthquake of January 17, 1994, *Earth Reinforcement*, (eds. by Ochiai et al.), Balkema, **2**, 965–974.

## APPENDIX A: SIMILITUDE ANALYSIS OF THE NATURAL FREQUENCIES OF THE MODELS

The shear modulus of unbound granular materials is proportional to $\sigma^n$, where $\sigma$ is the confining pressure and $n$ is the power. It was anticipated that the strain in the backfill would become around 0.01% at the start of shaking and then to the order of 1% when the model is shaken largely during the major period of test. When the strain level increases from 0.01% to 1.0%, the power $n$ for unbound granular materials increases from about 0.5 to about 1.0 (Iwasaki et al., 1978).

Conversely, the natural frequency $f_n$ of respective model is proportional to $\lambda^{(1+n)/2}$ times as large as the value of the corresponding prototype, where $\lambda$ is the ratio of length between the prototype and the model (*see* Appendix B). For the considered value of $\lambda$ (equal to six), the value of $\lambda^{(1+n)/2}$ becomes equal to $\lambda^{3/4}=3.8$ (when the strain level is low, around 0.01%) and $\lambda=6$ (when the strain level is high, of the order of 1%). Therefore, to achieve a ratio between the $f_n$ value of model structure and the frequency $f_i$ of input motion that is similar to the one with the considered prototype structures, the frequency $f_i$ of input motion to be used in the present model tests should be:

a) about 3.8 times the estimated predominant frequency $f_p=1$–3 Hz for the 1995 Hyogoken-Nambu Earthquake (i.e., $f_i \approx 3.8$–11 Hz) to simulate the behaviour at relatively low strain levels (of the order of 0.01%); and
b) about 6 times 1–3 Hz (i.e., $f_i \approx 6$–18 Hz) to simulate the behaviour at relatively large strains (of the order of 1%).

The values $f_i=5$ Hz and 10 Hz employed in the present study are within the range of frequency shown above (*see* Table 1) and therefore were adequate to achieve realistic dynamic behaviour of the considered prototype structures in present model tests.

## APPENDIX B: SIMILITUDE FOR DYNAMIC BEHAVIOUR OF MODEL

The $1/\lambda$-scale models used in the present study satisfy the following considered conditions (Rocha, 1957):

**Table 1. Relationships between the input or predominant frequency and the natural frequency of structure between the model and the conceived prototype structures**

| Model tests | | | Considered prototype structures with $\lambda=6$ | |
|---|---|---|---|---|
| Input frequency $f_i$ estimated by the similitude rule based on $f_p=1-3$ Hz of the actual earthquake | Actually used input frequency $f_i$ (Hz) | Measured natural frequency $f_n$ (Hz) at small strains (when PS = 15 – 45 kPa) | Predominant frequency $f_p$ (Hz) during the Hyogoken-Nambu Earthquake | Natural frequency $f_n$ (Hz) at small strains estimated from the value measured with a prototype structure |
| 3.8 – 11 for small strain behaviour; and 6 – 18 for large strain behaviour | 5 | 10 – 12 | 1 – 3 | 4.6 – 6.2 (this value would decrease and approach $f_p$ when the prestress is largely lost). |
| | 10 | | | |

$$l_m=(1/\lambda)\cdot l_p \tag{B1}$$

$$\sigma_{c\cdot m}=(1/\lambda)\cdot\sigma_{c\cdot p} \tag{B2}$$

where $l$ is the length; $\sigma_c$ is the confining pressure; and the subscripts $m$ and $p$ denote model and prototype. The following predominant physical laws were considered:
Gravitational force:

$$F_g=\rho\cdot g\cdot l^3 \text{ ($g$: the gravity acceleration)} \tag{B3}$$

Shear resistance along shear bands:

$$F_s=\sigma_n\cdot\tan\phi\cdot l^2 \text{ ($\phi$: the friction angle of backfill)} \tag{B4}$$

Normal force on shear bands:

$$F_N=\sigma_n\cdot l^2 \text{ ($\sigma_n$: the normal stress on shear bands)} \tag{B5}$$

Friction between facing and backfill:

$$F_p=\sigma_n\cdot\tan\delta\cdot l^2 \tag{B6}$$

Tie rod tension:

$$F_c=E\cdot l^2\cdot\varepsilon=K_t\cdot\varepsilon_t \tag{B7}$$

Inertia force of model:

$$F_i=M\cdot f^2\cdot l=\rho\cdot f^2\cdot\gamma\cdot l^4;\ \text{or}\ F_i=M\cdot\alpha=\alpha\cdot\rho\cdot l^3 \tag{B8}$$

where $\alpha$ is the response acceleration of model; $\rho$ is the density of backfill; $\delta$: the friction angle at the interface between the facing and the backfill; $E$ is the Young's modulus of tie rod; $f$ is the frequency of shaking; and $\gamma$ is the shear strain of model.

The following seven $\pi$ terms (dimensionless), which are the ratios of the predominant factors ($F_g$, $F_S$, $F_N$, $F_P$, $F_c$ and $F_i$) to external force ($F$), were considered:

$$\pi_1=\frac{F_S}{F_g}=\frac{\sigma_n\cdot\tan\phi\cdot l^2}{\rho\cdot g\cdot l^3};\quad \pi_2=\frac{F_N}{F_g}=\frac{\sigma_n\cdot l^2}{\rho\cdot g\cdot l^3};$$

$$\pi_3=\frac{F_P}{F_g}=\frac{\sigma_n\cdot\tan\delta\cdot l^2}{\rho\cdot g\cdot l^3};\quad \pi_4=\frac{F_c}{F_g}=\frac{K_t\cdot\varepsilon_t}{\rho\cdot g\cdot l^3};$$

$$\pi_5=\frac{F_i}{F_g}=\frac{\rho\cdot f_2\cdot\gamma\cdot l^4}{\rho\cdot g\cdot l^3};\quad \pi_6=\frac{F_i}{F_g}=\frac{\alpha\cdot\rho\cdot l^3}{\rho\cdot g\cdot l^3};$$

$$\text{and}\ \pi_7=\frac{F}{F_g}=\frac{F}{\rho\cdot g\cdot l^3}$$

On the other hand, the shear strain $\gamma=\tau/G$ is proportional to $(\sigma_c)^n$, where $\sigma_c$ is the confining pressure and the $n$ is the power. Referring to Eq. (B2), we obtain:

$$\gamma_p/\gamma_m=\sigma^n_{c\cdot p}/\sigma^n_{c\cdot m}=\lambda^n \tag{B9}$$

Substituting Eq. (B9) into $\pi_5=F_i/F_g=(\rho\cdot f^2\cdot\gamma\cdot l^4)/(\rho\cdot g\cdot l^3)$, the ratio of frequency between model and prototype is obtained as:

$$f_m/f_p=\lambda^{\frac{n+1}{2}} \tag{B10}$$

The scaling factors between model and prototype for the other quantities that were obtained as above are listed below:

**Table 2.**

| Parameter | Symbol | Scaling factor (model/prototype) |
|---|---|---|
| Gravity | $g$ | 1 |
| Acceleration | $\alpha$ | 1 |
| Unit weight of the soil | $\rho$ | 1 |
| Stress | $\sigma$ | $1/\lambda$ |
| Frequency | $\omega$ | $\lambda^{(n+1)/2}$ |
| Strain | $\varepsilon$ | $1/\lambda^n$ |

## APPENDIX C: EQUATION OF MOTION FOR A SDOF SYSTEM

The equation of motion for a linear damped single-degree-of-freedom system is obtained as:

$$m\ddot{z}+c\dot{y}+ky=0 \tag{C1}$$

where $m$ is the mass; $z$ is the absolute displacement; $c$ is the Newton's viscosity coefficient; $k$ is the linear spring constant; and $y$ is the relative displacement of structure. By substituting $z=x+y$ into Eq. (C1), after some rearrangements, we obtain the following equation for the simple harmonic loading $x=x_0\cdot\cos\omega t$:

$$\ddot{y}+2hn\dot{y}+n^2y=\omega^2\cdot x_0\cos\omega t \tag{C2}$$

where $h=c/(2\sqrt{mk})$ and $n^2=k/m$. The steady-state response after the transient response dies out is given as:

$$y=\frac{\omega^2\cdot x_0}{n^2}\frac{1}{\sqrt{\{1-(\omega/n)^2\}^2+4h^2(\omega/n)^2}}\cos(\omega t-\varphi_1) \quad \text{(C3)}$$

By substituting the values of $y$ and $\dot{y}$ from Eq. (C3) into Eq. (C2), we obtain:

$$\ddot{x}+\ddot{y}=-\omega^2\cdot x_0\cdot L\cdot\cos(\omega t-\varphi) \quad \text{(C4)}$$

where $L$ is the ratio of the response acceleration of structure to the input acceleration $\omega^2\phi_0$ to and $\varphi$ is the phase angle. By substituting $n=f_n$ and $\omega=f_i$ into Eq. (C4), $L$ and $\varphi$ can be expressed as Eqs. 1(a) and 1(b).

## APPENDIX D: A SIMPLIFIED METHOD TO DERIVE THE NATURAL FREQUENCY OF STRUCTURE

When based on the three assumptions listed in the first paragraph of Section "ESTIMATION OF THE NATURAL FREQUENCY OF STRUCTURE", the total kinetic energy by horizontal displacement and rotation of both the backfill (as an elastic beam) and the top plate (as a rigid mass) during shaking is given as:

$$K(t)=\frac{1}{2}\cdot m\cdot\dot{u}_1^2+\int_0^H\frac{1}{2}\cdot\frac{M}{H}\cdot\dot{u}_2^2dx+\int_0^H\frac{1}{2}\cdot I_2\cdot\dot{\theta}_2^2dx \quad \text{(D1)}$$

where $u_1$ and $u_2$ are the horizontal displacement of the top plate and of the elastic beam (as a function of $x$), respectively; $I_2$ is the moment of inertia of the elastic beam; and $\theta_2$ is the rotation angle (as a function of $x$) of the elastic beam. The maximum value of $K(t)$ is obtained as:

$$K_{max}=\frac{\omega^2P^2}{840E^2G^2B_2^6B_3^2}\{\alpha_1+7B_2^2(\alpha_2+5kEB_2^2(\alpha_3+\alpha_4))\} \quad \text{(D2)}$$

where $k$ is a constant value depending on the cross-sectional shape of backfill ($k=1.5$ in the present case); $\alpha_1=48G^2H^6(35m+27M)$; $\alpha_2=4GH^4\{6GM+kE\,(60m+41M)\}$; $\alpha_3=4H^2\{GM+kE(3m+2M)\}$; and $\alpha_4=KEMB_2^2$.

On the other hand, by assuming that the strain energy induced by the moment $M_m$ and the shear force $Q$ is predominant for the elastic beam, the total strain energy $U$ is obtained as:

$$U(t)=\frac{1}{2}\int_0^H\left(\frac{M_m^2}{EI}+\kappa\frac{Q^2}{GA}\right)dx \quad \text{(D3)}$$

where $I$ is the moment of inertia of the cross-sectional area $A$ of the elastic beam; and $\kappa$ is the constant depending on its shape of cross section ($\kappa=1.2$ in the present case). The maximum strain energy is obtained as:

$$U_{max}=\frac{2P^2H(12\kappa+GB_2B_3H^2)}{EGB_2^4B_3^2} \quad \text{(D4)}$$

By equating Eqs. (D2) and (D4), the natural frequency is obtained as:

$$f_n=\frac{2}{\pi}\sqrt{\frac{\zeta_1}{\zeta_2+7B_2^2\{\zeta_3+5kEB_2^2(\zeta_4+\zeta_5)\}}} \quad \text{(D5)}$$

where $\zeta_1=105EGB_2^2H\,(12\kappa+GB_2B_3H^2)$; $\zeta_2=48G^2H^6(35m+27M)$; $\zeta_3=4GH^4\{6GM+kE\,(60m+41M)\}$; $\zeta_4=4H^2\{GM+kE\,(3m+2M)\}$; and $\zeta_5=kEMB_2^2$.